Crucial Role of ROCK2 in Vascular Smooth Muscle Cells for Hypoxia-Induced Pulmonary Hypertension in Mice

Toru Shimizu, Yoshihiro Fukumoto, Shin-ichi Tanaka, Kimio Satoh, Shohei Ikeda, Hiroaki Shimokawa

Objective—Rho/Rho-kinase (ROCK) pathway in vascular smooth muscle cells (VSMCs) plays an important role in the pathogenesis of cardiovascular diseases, including pulmonary arterial hypertension (PAH). Rho-kinase has 2 isoforms, ROCK1 and ROCK2, with different functions in different cells; ROCK1 for circulating inflammatory cells and ROCK2 for the vasculature. In the present study, we aimed to examine whether ROCK2 in VSMC is involved in the pathogenesis of PAH.

Approach and Results—In patients with PAH, the expression of ROCK2 was increased in pulmonary arterial media and primary pulmonary arterial smooth muscle cells when compared with controls. To investigate the role of ROCK2 in VSMC, we generated VSMC-specific heterozygous ROCK2-deficient ($ROCK2^{+/-}$) mice and VSMC-specific ROCK2-overexpressing transgenic (ROCK2-Tg) mice. The extent of hypoxia-induced pulmonary hypertension was reduced in $ROCK2^{+/-}$ mice and was enhanced in ROCK2-Tg mice compared with respective littermates. The protein expression of ROCK activity and phosphorylated extracellular signal–regulated kinase and the number of Ki67-positive proliferating cells in the lung were reduced in $ROCK2^{+/-}$ mice and were increased in ROCK2-Tg mice compared with respective littermates. In cultured mouse aortic VSMC, migration and proliferation activities were reduced in $ROCK2^{+/-}$ mice, and migration activity was increased in ROCK2-Tg mice compared with respective littermates. In addition, in primary pulmonary arterial smooth muscle cells from a patient with PAH, ROCK2 was required for migration and proliferation through ROCK and extracellular signal–regulated kinase activation.

Conclusions—ROCK2 in VSMC contributes to the pathogenesis of PAH. **(*Arterioscler Thromb Vasc Biol*. 2013;33:2780-2791.)**

Key Words: hypertension, pulmonary ■ muscle, smooth, vascular ■ rho-associated kinase

Pulmonary arterial hypertension (PAH) is a fatal disease characterized by increased pulmonary vascular resistance, leading to right heart failure and death.[1,2] Increased pulmonary vascular resistance is caused by distal pulmonary vascular remodeling, including prolonged vasoconstriction, proliferation and migration of vascular smooth muscle cells (VSMCs), and endothelial injury.[3] Although multiple pharmacological agents, such as vasodilators and anticoagulants, have been developed for the treatment of PAH, long-term prognosis of patients with severe PAH remains poor because of progressive right heart failure.[3] Thus, more effective treatments need to be urgently developed.

Rho-kinase (ROCK) belongs to the serine/threonine kinases family and is an important downstream effector of the small GTP-binding protein RhoA. It has been demonstrated that Rho/ROCK pathway plays an important role in various fundamental cellular functions, including contraction, motility, proliferation, and migration, leading to the development of cardiovascular diseases, including PAH.[4,5] There are 2 isoforms of ROCK: ROCK1 (Rho-kinase β) and ROCK2 (Rho-kinase α).[6] ROCK1 and ROCK2 are highly homologous, sharing 65% homology in amino acid sequence and 92% homology in their kinase domains.[6] Both isoforms are ubiquitously expressed in invertebrates and vertebrates with ROCK1 expressed mainly in circulating inflammatory cells and ROCK2 in VSMC.[7,8] Homozygous ROCK1-deficient mice show open eyelids at birth and omphalocele, whereas homozygous ROCK2-deficient mice die embryonically because of placental dysfunction,[9,10] suggesting that ROCK1 and ROCK2 mediate different functions in different types of cells.

We have previously reported that a long-term treatment with an isoform-nonspecific ROCK inhibitor, fasudil, suppresses the development of monocrotaline-induced and hypoxia-induced pulmonary hypertension (PH) in animal models.[11,12] Furthermore, we have recently obtained a direct evidence for increased ROCK activation in patients with idiopathic PAH (IPAH).[13] However, although isoform-nonspecific ROCK inhibitors were effective in previous studies of PAH in both animals and humans,[14] the particular isoform of ROCK responsible for the effect has not been evaluated.

It was previously reported that heterozygous ROCK1-deficient mice had decreased neointima formation after carotid artery ligation associated with reduced leukocyte-mediated inflammation.[15] Thus, ROCK1 seems to play an important role in circulating inflammatory cells in the pathogenesis of vascular diseases.[7,8] In contrast, Rho/ROCK2 pathway plays a central role in VSMC-mediated vasoconstriction

Received on: February 13, 2013; final version accepted on: September 30, 2013.

From the Department of Cardiovascular Medicine, Tohoku University Graduate School of Medicine, Sendai, Japan.

This manuscript was sent to Karin Bornfeldt, Consulting Editor, for review by expert referees, editorial decision, and final disposition.

The online-only Data Supplement is available with this article at http://atvb.ahajournals.org/lookup/suppl/doi:10.1161/ATVBAHA.113.301357/-/DC1.

Correspondence to Hiroaki Shimokawa, MD, PhD, Department of Cardiovascular Medicine, Tohoku University Graduate School of Medicine, 1-1 Seiryocho, Aoba-ku, Sendai 980-8574, Japan. E-mail shimo@cardio.med.tohoku.ac.jp

Nonstandard Abbreviations and Acronyms	
ERK	extracellular signal–regulated kinase
HO-1	heme oxygenase-1
PAH	pulmonary arterial hypertension
PASMCs	pulmonary arterial smooth muscle cells
PH	pulmonary hypertension
ROCK	Rho-kinase
RV	right ventricle
VSMCs	vascular smooth muscle cells

that promotes PAH, where ROCK2 predominantly regulates VSMC contractility when compared with ROCK1, by directly binding to and phosphorylating the myosin-binding subunit of myosin phosphatase.[16] However, the role of ROCK2 remains largely unknown in the pathogenesis of PAH characterized by increased vasoconstriction, proliferation, and migration of VSMC. Furthermore, no study has ever used genetically modified mouse models to identify the role of ROCK2 in PAH. In the present study, we thus developed VSMC-specific heterozygous ROCK2-deficient (ROCK2$^{+/-}$) mice using the Cre-loxP system and VSMC-specific ROCK2-overexpressing transgenic (ROCK2-Tg) mice under the control of *SM22*α promoter (Figure IA–IC in the online-only Data Supplement) and adopted a mouse model of hypoxia-induced PH.[17] Using these mouse models, we tested our hypothesis; when compared with ROCK1, ROCK2 in VSMC contributes to the pathogenesis of PAH through enhanced VSMC migration and proliferation.

Materials and Methods

Materials and Methods are available in the online-only Supplement.

Results

Upregulation of ROCK2 in the Media of Pulmonary Arteries and PASMC From Patients With IPAH

First, we examined whether the expression of ROCK2 is upregulated in lung tissues and pulmonary arterial smooth muscle cells (PASMCs) from patients with IPAH. Immunostaining of ROCKs showed that immunoreactivity of ROCK2, but not that of ROCK1, was enhanced in the pulmonary arteries from patients with IPAH compared with controls (Figure 1A). Furthermore, the enhanced expression of ROCK2 was colocalized with α-smooth muscle actin–positive pulmonary arterial media composed of PASMC (Figure 1A). The number of proliferating and inflammatory cells coexpressing phosphorylated form of extracellular signal–regulated kinase 1/2 (P-ERK 1/2), Ki67, and CD45 was also markedly increased around the pulmonary arteries from patients with IPAH (Figure II in the online-only Data Supplement). Reverse transcriptase-polymerase chain reaction also showed the upregulation of *ROCK2*, but not *ROCK1*, in PASMC from pulmonary arteries of IPAH patients as compared with controls (Figure 1B and 1C).

Attenuation of Hypoxia-Induced PH in VSMC-Specific ROCK2-Deficient Mice

Next, we performed an in vivo study, using the mouse model of hypoxia-induced PH in ROCK2$^{+/-}$ mice and littermate controls

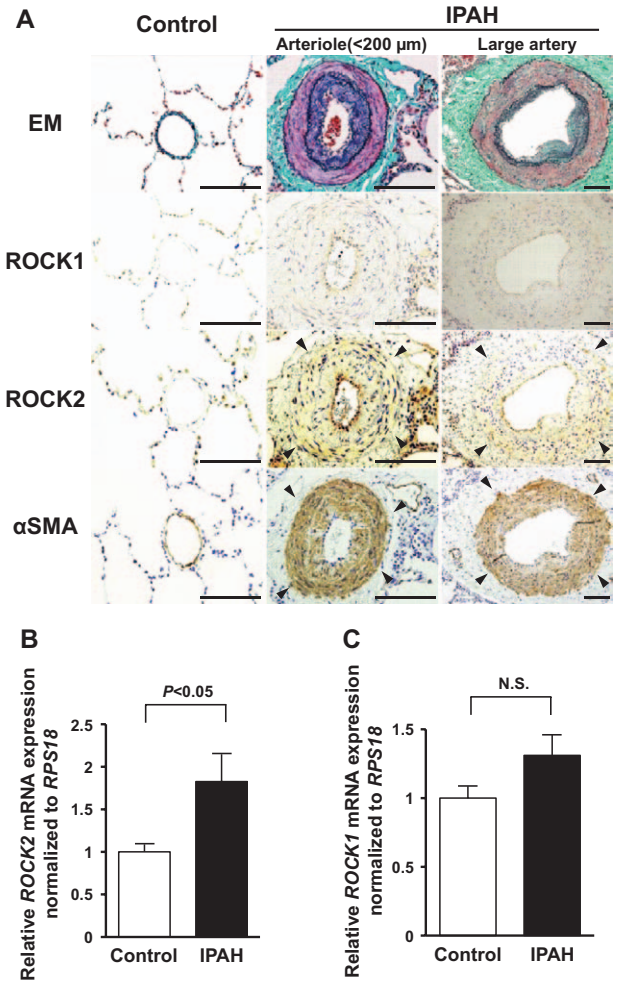

Figure 1. Rho-kinase 2 (ROCK2) expression is enhanced in the media of pulmonary arteries and pulmonary arterial smooth muscle cells (PASMC) from patients with idiopathic pulmonary arterial hypertension (IPAH). **A**, Representative serial lung sections stained with Elastica-Masson (EM) and immunostained with antibodies to ROCK1, ROCK2, and α-smooth muscle actin (αSMA). Arrowheads show strong coexpression of ROCK2 and αSMA in the media of pulmonary arterioles (<200 μm) and large arteries from patients with IPAH compared with controls who underwent operation for lung cancer. Scale bars=100 μm. **B** and **C**, Reverse transcriptase-polymerase chain reaction analysis of *ROCK1* and *ROCK2* mRNA expression in PASMC from patients with IPAH (n=5) and controls (n=5).

(LM), both of which showed normal growth under physiological conditions. When compared with aortic VSMC from LM (LM VSMC), mRNA (reverse transcriptase-polymerase chain reaction) and protein (Western blotting) expressions of ROCK2 in aortic VSMC from ROCK2$^{+/-}$ mice (ROCK2$^{+/-}$ VSMC) were significantly reduced by 42% and 24%, respectively. In contrast, the expressions of ROCK1 in VSMC were comparable between the 2 genotypes (Figure IIIA–IIIE in the online-only Data Supplement). In addition, we confirmed that the protein expression of ROCK2 in the denuded aorta was reduced in ROCK2$^{+/-}$ compared with LM mice (Figure IIIF–IIIH in the online-only Data Supplement). After long-term exposure to hypoxia (10% O_2 for 4 weeks), hemoglobin concentration was significantly elevated in both ROCK2$^{+/-}$ and LM mice to the same extent (19.9 versus 19.5 g/dL, respectively), platelet count

was also significantly decreased to the same extent (417×10^3 versus 425×10^3 mm^3, respectively; Table I in the online-only Data Supplement), and no difference in the pulmonary vasculature was noted between the 2 genotypes under normoxic conditions. Similarly, chronic hypoxia prevented the body weight gain to the same extent between the 2 genotypes (Figure IVA in the online-only Data Supplement). Under normoxic conditions, right ventricular systolic pressure was comparable between the 2 genotypes. However, after hypoxic exposure, the elevation of RV systolic pressure was significantly suppressed in ROCK2$^{+/-}$ compared with LM mice (Figure 2A; Table 1). Although other RV hemodynamic parameters, such as RV end-diastolic pressure and peak rates of RV pressure development (RV dP/dt max) and relaxation (RV dP/dt min), were comparable between the 2 genotypes under normoxic conditions, hypoxia-induced increases in those parameters were also significantly suppressed in ROCK2$^{+/-}$ than in LM mice (Figure 2A; Table 1). In contrast, there was no significant difference in heart rate, systemic blood pressure, or left ventricular hemodynamic parameters between the 2 genotypes before and after chronic hypoxia (Table 1). The extent of RV hypertrophy, as measured by the ratio of RV/(left ventricle+septum [S]), was also significantly less in ROCK2$^{+/-}$ compared with LM mice after chronic hypoxia (Figure 2B). Furthermore, histological analysis showed that the extent of hypoxia-induced pulmonary vascular remodeling was significantly suppressed in ROCK2$^{+/-}$ compared with LM mice (Figure 2C and 2D). The number of CD45-positive inflammatory cells in the hypoxic pulmonary artery was also significantly reduced in ROCK2$^{+/-}$ compared with LM mice (Figure 2E and 2F). These results indicate that ROCK2 deficiency in VSMC ameliorates hypoxia-induced PH in mice in vivo.

Augmentation of Hypoxia-Induced PH in VSMC-Specific ROCK2-Overexpressing Mice

We then performed an in vivo study, using the mouse model of hypoxia-induced PH in ROCK2-Tg and wild-type littermate controls (CTL), both of which showed normal growth under physiological conditions. Protein expressions of ROCK2 in both VSMC and the whole aorta were significantly increased in ROCK2-Tg mice by 186% and 137%, respectively, with no changes in ROCK1 expression (Figure VA, VB, VC, VF, VG, and VH in the online-only Data Supplement) compared with those of CTL mice. This was also the case for reverse transcriptase-polymerase chain reaction in VSMC (Figure VD and VE in the online-only Data Supplement). Chronic hypoxia significantly increased hemoglobin concentration, decreased platelet count, and prevented body weight gain to the same extent in ROCK2-Tg and CTL mice (Table II in the online-only Data Supplement; Figure IVB in the online-only Data Supplement). Although all RV hemodynamic parameters were comparable between the 2 genotypes under normoxic conditions, hypoxia-induced increase in RV systolic pressure was significantly enhanced in ROCK2-Tg compared with CTL mice under hypoxic conditions (Figure 3A; Table 2). In contrast, there was no significant difference in heart rate, systemic blood pressure, or left ventricular hemodynamic parameters between the 2 genotypes before and after chronic hypoxia (Table 2). The extent of hypoxia-induced RV hypertrophy, pulmonary vascular remodeling, and inflammation was significantly enhanced in ROCK2-Tg compared with CTL mice (Figure 3B–3F). These results indicate that ROCK2 overexpression in VSMC promotes hypoxia-induced PH in mice in vivo.

Role of ROCK2 in Hypoxia-Induced Pulmonary Vascular Cell Proliferation In Vivo

To further elucidate the mechanism of ROCK2-mediated development of hypoxia-induced PH in mice, we evaluated pulmonary vascular cell proliferation by immunostaining of Ki67 and P-ERK 1/2. The number of Ki67-positive cells was significantly reduced in ROCK2$^{+/-}$ compared with LM mice (Figure 4A and 4B). Furthermore, immunostaining and Western blot of lung tissues showed that hypoxia-induced increase in ERK activity (ratio of P-ERK1/2 to total ERK1/2) in LM mice was significantly suppressed in ROCK2$^{+/-}$ mice (Figure 4C–4E). Similarly, the whole ROCK activity (extent of phosphorylation of the myosin-binding subunit) of lung tissues was markedly increased in LM mice after chronic hypoxia and was significantly attenuated in ROCK2$^{+/-}$ mice (Figure 4D and 4F). In contrast, in ROCK2-Tg mice, the hypoxia-induced increases in the number of Ki67-positive cells and those in ERK and ROCK activities of lung tissues were significantly enhanced compared with CTL mice (Figure 4G–4L). These results indicate that ROCK2 in PASMC contributes to the pathogenesis of hypoxia-induced PH, at least in part, through enhanced pulmonary vascular cell proliferation in vivo.

Role of ROCK2 in VSMC Proliferation and Migration In Vitro

VSMC proliferation and migration are typical characteristics of PH.[18] To further elucidate the role of ROCK2 in PAH, we performed cell proliferation and migration assay in vitro using the aortic VSMC cultured from each genotype of mice. VSMC proliferation, as measured by cell number in response to 10% or 0.1% fetal bovine serum, was significantly decreased in ROCK2$^{+/-}$ compared with LM mice (Figure 5A and 5B), whereas it was comparable between ROCK2-Tg and CTL mice (Figure 5C and 5D). In addition, to evaluate VSMC migration, we performed both scratch and a modified Boyden chamber assays. VSMC migration, as assessed by scratch assay in response to 0.1% fetal bovine serum, was significantly reduced in ROCK2$^{+/-}$ mice (Figure 5E and 5F) and was significantly enhanced in ROCK2-Tg mice (Figure 5G and 5H) compared with respective littermates. Similar results were also obtained with a modified Boyden chamber assay in response to platelet-derived growth factor (Figure 5I–5 L). Consistent with these findings, Western blot showed that ERK activity in VSMC after platelet-derived growth factor stimulation was significantly reduced in ROCK2$^{+/-}$ mice, whereas it increased in ROCK2-Tg mice compared with respective littermates (Figure VIA–VID in the online-only Data Supplement).

ROCK2-Induced Oxidative Stress and Inflammation in VSMC

To further elucidate the mechanism of VSMC proliferation, we performed analyses with VSMC from each genotype of mice (Figures VII and VIII in the online-only Data Supplement).

First, we examined the expression of oxidative stress genes in VSMC because they play an important role in VSMC

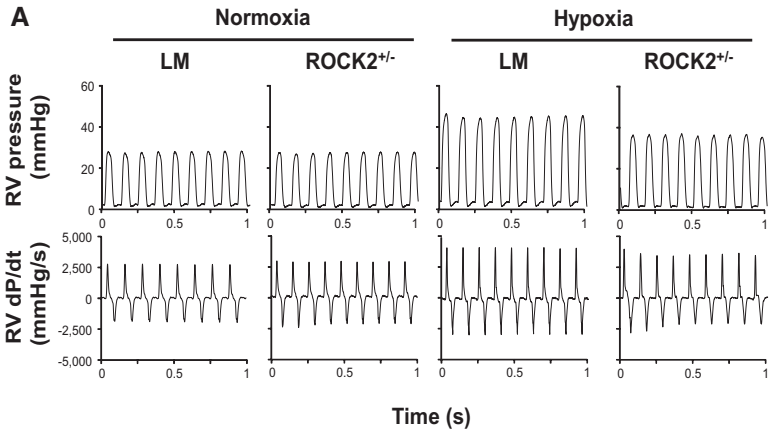

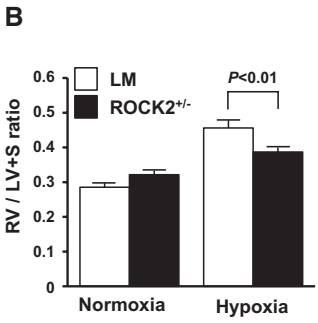

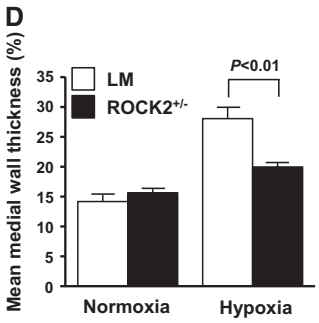

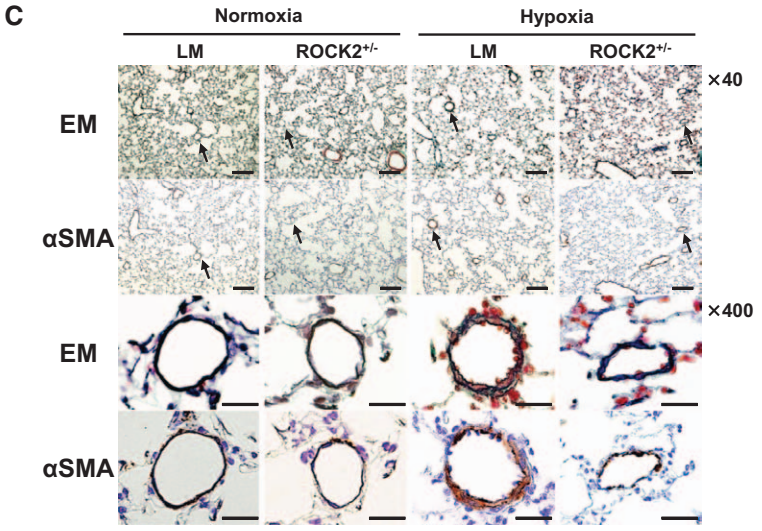

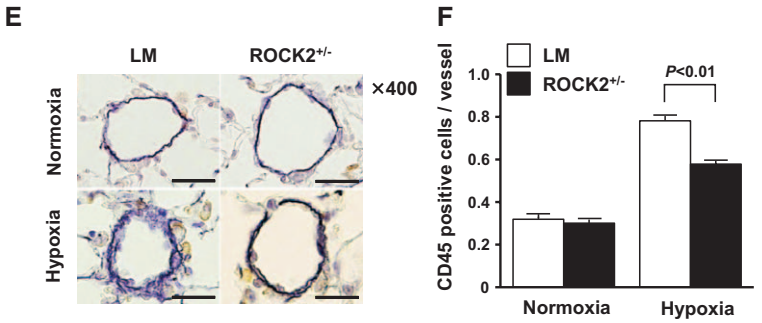

Figure 2. Rho-kinase 2 (ROCK2) deficiency in vascular smooth muscle cells (VSMC) attenuates hypoxia-induced pulmonary hypertension and pulmonary vascular remodeling. **A**, Representative tracings of right ventricular (RV) pressure and dP/dt, measured by right heart catheterization. VSMC-specific heterozygous ROCK2-deficient mice (ROCK2$^{+/-}$) and littermate control mice (LM) were exposed to room air (normoxia) or 10% oxygen (hypoxia) for 4 weeks. **B**, RV hypertrophy assessed by the ratio of RV weight to left ventricular (LV) plus septum (S) weight (RV/LV+S) after exposure to normoxia or hypoxia for 4 weeks (n=15 each). **C**, Representative serial sections of pulmonary arterioles stained with Elastica-Masson (EM) and with antibodies to α-smooth muscle actin (αSMA) exposed to normoxia or hypoxia for 4 weeks. Scale bars represent 100 μm (×40 magnification) and 25 μm (×400 magnification). **D**, Pulmonary vascular remodeling assessed by percentage medial wall thickness of pulmonary arterioles (n=6–8 each). **E**, Representative serial sections of pulmonary arterioles immunostained with antibodies to CD45 exposed to normoxia or hypoxia for 4 weeks. Scale bars=25 μm. **F**, The number of CD45-positive inflammatory cells per pulmonary arterioles (n=5 each). Results are expressed as mean±SEM.

proliferation and PH development.[18] Inconsistent with the previous reports that ROCK contributes to oxidative stress induction in VSMC, the expression of NADPH oxidases (eg, NOX2 and NOX4) was lower in *Rock2*$^{+/-}$ than that in *Rock2*$^{+/+}$ VSMC under both normoxic and hypoxic conditions (Figure VIIA and VIIC in the online-only Data Supplement). In contrast, the

Table 1. Hemodynamic Variables in Littermate Control (LM) and VSMC-Specific ROCK2-Deficient (ROCK2$^{+/-}$) Mice Under Normoxia and After 4-wk Hypoxia

	Normoxia		Hypoxia	
Parameters	LM (n=10)	ROCK2$^{+/-}$ (n=10)	LM (n=10)	ROCK2$^{+/-}$ (n=10)
Heat rate, beats/min	510±19	491±19	509±15	506±20
RVSP, mm Hg	29.4±0.7	29.3±0.8	43.9±1.5**	38.9±0.7**††
RVEDP, mm Hg	0.9±0.1	1.0±0.2	1.6±0.1**	1.1±0.1**†
RV dP/dt max, mm Hg/s	3060±211	3138±220	4143±273**	3306±154**†
RV dP/dt min, mm Hg/s	1898±142	1833±108	3282±218**	2616±94**†
Systolic blood pressure, mm Hg	104±4	103±2	101±4	99±4
Diastolic blood pressure, mm Hg	72±3	70±3	70±4	69±2
LVSP, mm Hg	107±4	102±4	106±4	103±5
LVEDP mm Hg	5.5±0.6	5.1±0.7	5.3±0.8	5.0±0.5
LV dP/dt max, mm Hg/s	10764±1296	11312±829	9775±881	9140±620
LV dP/dt min, mm Hg/s	7325±552	7545±740	9015±923	8072±601

Results are expressed as mean±SEM. Comparisons were performed using 1-way ANOVA. LV dP/dt max indicates peak rates of left ventricular pressure development; LV dP/dt min, peak rates of LV pressure relaxation; LVEDP, LV end-diastolic pressure; LVSP, left ventricular systolic pressure; ROCK, Rho-kinase; RV dP/dt max, peak rates of right ventricular pressure development; RV dP/dt min, peak rates of RV pressure relaxation; RVEDP, RV end-diastolic pressure; RVSP, right ventricular systolic pressure; and VSMC, vascular smooth muscle cells.

**P<0.01 vs normoxia in each group.

†P<0.05.

††P<0.01 vs hypoxic LM mice.

expression of these NADPH oxidases was significantly higher in aortic VSMC from ROCK2-Tg mice (ROCK2-Tg VSMC) than in those from littermate control mice (CTL VSMC) under both normoxic and hypoxic conditions (Figure VIIB and VIID in the online-only Data Supplement). Second, because heme oxygenase-1 (HO-1) is well-known to have protective effects against oxidative stress, we analyzed HO-1 mRNA expression in the same manner. HO-1 was significantly induced in *Rock2*$^{+/-}$ when compared with *Rock2*$^{+/+}$ VSMC under both normoxic and hypoxic conditions (Figure VIIE in the online-only Data Supplement). In contrast, the expression of HO-1 was significantly less in ROCK2-Tg VSMC than that in CTL VSMC under normoxic conditions (Figure VIIF in the online-only Data Supplement), suggesting that the HO-1 expression is specifically regulated by ROCK2 in VSMC. These data are consistent with the established role of HO-1 that inhibits VSMC proliferation.[19] Third, we performed analysis on the expression of adhesion molecule in these VSMC. Vascular cell adhesion molecule-1 was inhibited in *Rock2*$^{+/-}$ compared with *Rock2*$^{+/+}$ VSMC under both normoxic and hypoxic conditions (Figure VIIG in the online-only Data Supplement). In contrast, the expression of vascular cell adhesion molecule-1 was significantly increased in ROCK2-Tg VSMC than that in CTL VSMC under both normoxic and hypoxic conditions (Figure VIIH in the online-only Data Supplement), suggesting that the expression of vascular cell adhesion molecule-1 was strongly regulated by ROCK2 in VSMC.

We further examined the secretion of inflammatory cytokines from VSMC in vitro. The levels of inflammatory cytokines (eg, interferon-γ and tumor necrosis factor-α) secreted by VSMC were significantly reduced in ROCK2$^{+/-}$ VSMC and increased in ROCK2-Tg VSMC compared with control VSMC under both normoxic and hypoxic conditions (Figure VIIIA–VIIID in the online-only Data Supplement). Because interferon-γ and tumor necrosis factor-α contribute to VSMC proliferation and migration,[20,21] ROCK2 may contribute to VSMC proliferation and migration through autocrine/paracrine mechanisms by secreting these cytokines.

Knockdown of ROCK2 in PASMC From a Patient With IPAH

Finally, to determine whether ROCK2 rather than ROCK1 plays important roles in human PAH, PASMCs were isolated from pulmonary arteries from a patient with IPAH (IPAH-PASMC) who underwent lung transplantation. We also examined the role of each ROCK isoform in those cells using small interfering RNA (siRNA) knockdown technique. Western blot showed that the transfection of *ROCK1*- and *ROCK2*-siRNA to IPAH-PASMC reduced the expression of each isoform by 70% and 81%, respectively, compared with control siRNA, without affecting the protein expression of another isoform (Figure IXA in the online-only Data Supplement). Effective knockdown was also confirmed at mRNA level by reverse transcriptase-polymerase chain reaction (Figure IXB–IXE in the online-only Data Supplement). Cell proliferation in response to 10% or 0.1% fetal bovine serum was significantly decreased in IPAH-PASMC transfected with *ROCK2*- and dual *ROCK1*/*2*-siRNA compared with control siRNA, whereas no such effect was noted with *ROCK1*-siRNA (Figure 6A and 6B). In contrast, cell migration, as assessed by scratch assay in response to 0.1% fetal bovine serum, was significantly reduced in IPAH-PASMC transfected with *ROCK1*-siRNA and those with *ROCK2*-siRNA to the same extent and was further suppressed in those with dual *ROCK1*/*2*-siRNA (Figure 6C and 6D). In addition, ROCK activity, as assessed by the ratio of phosphorylated myosin-binding subunit at thr853 but not at thr696 to total myosin-binding subunit, was significantly reduced in IPAH-PASMC transfected with *ROCK1*-, *ROCK2*-, and dual *ROCK 1*/*2*-siRNA compared with control siRNA (Figure 6E–6G). Finally, ERK activity in response to platelet-derived growth factor stimulation was significantly reduced in IPAH-PASMC transfected with *ROCK2*- and dual *ROCK1*/*2*-siRNA compared with control siRNA (Figure 6H and 6I). Taken together, these results indicate that ROCK2 rather than ROCK1 in human IPAH-PASMC mediates both cell proliferation and migration through ROCK activation and partially through ERK activation.

Discussion

The major findings of the present study are as follows: (1) the expression of ROCK2, but not ROCK1, was upregulated in the media of pulmonary arteries and PASMC from patients with IPAH; (2) ROCK2 in PASMC from mice was required for the development of hypoxia-induced PH; and (3) ROCK2

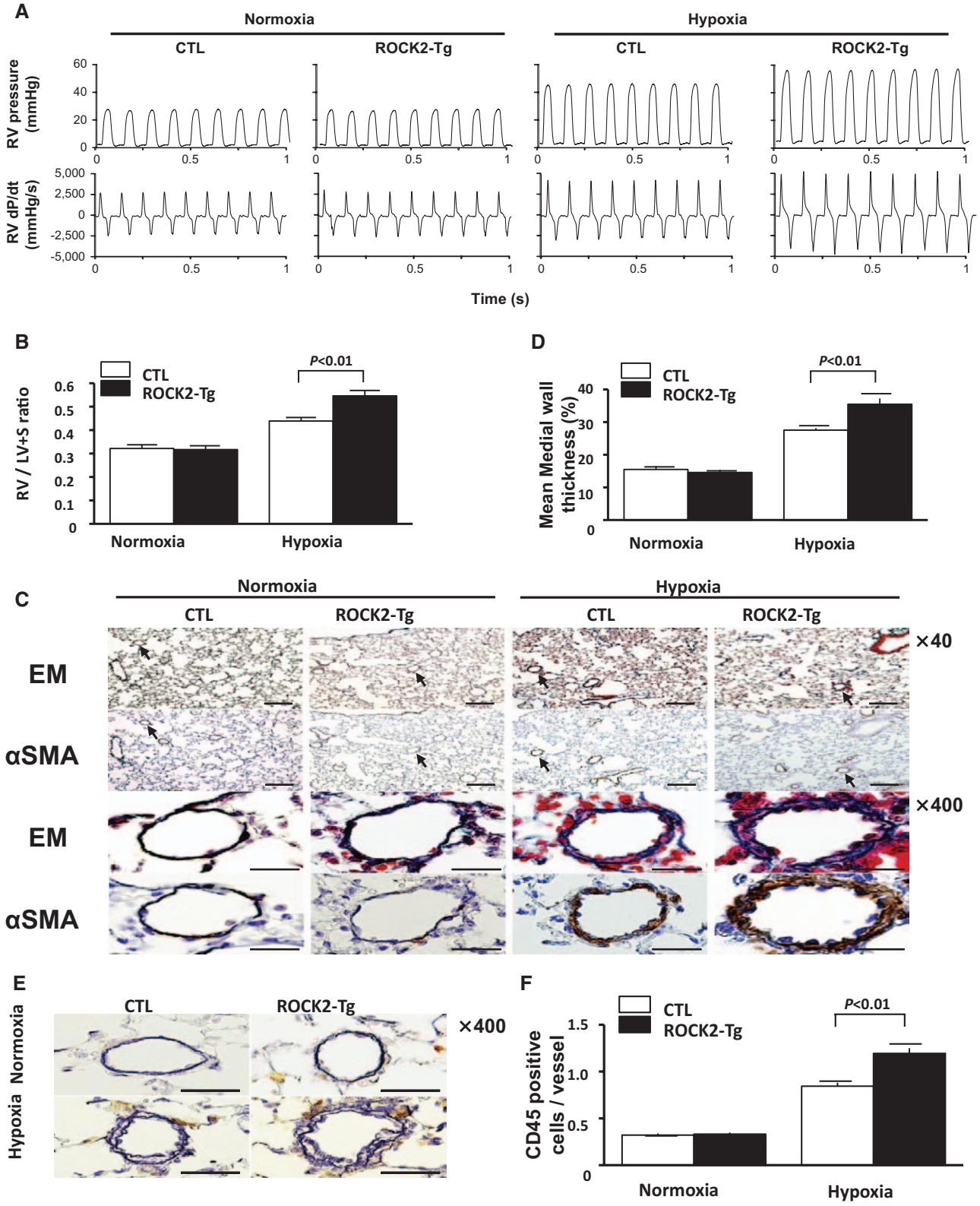

Figure 3. Rho-kinase 2 (ROCK2) overexpression in vascular smooth muscle cells (VSMC) augments hypoxia-induced pulmonary hypertension and pulmonary vascular remodeling. **A**, Representative tracings of right ventricular (RV) pressure and dP/dt measured by right heart catheterization. VSMC-specific ROCK2-overexpressing transgenic mice (ROCK2-Tg) and wild-type littermate control mice (CTL) were exposed to room air (normoxia) or 10% oxygen (hypoxia) for 4 weeks. **B**, RV hypertrophy assessed by the ratio of RV weight to left ventricular (LV) plus septum (S) weight (RV/LV+S) after exposure to normoxia or hypoxia for 4 weeks (n=15 each). **C**, Representative serial sections of pulmonary arterioles stained with Elastica-Masson (EM) and with antibodies to α-smooth muscle actin (αSMA) exposed to normoxia or hypoxia for 4 weeks. Scale bars represent 100 μm (×40 magnification) and 25 μm (×400 magnification). **D**, Pulmonary vascular remodeling assessed by percentage medial wall thickness of pulmonary arterioles (n=5–6 each). **E**, Representative serial sections of pulmonary arterioles immunostained with antibodies to CD45 exposed to normoxia or hypoxia for 4 weeks. Scale bars=25 μm. **F**, The number of CD45-positive inflammatory cells per pulmonary arterioles (n=5 each). Results are expressed as mean±SEM.

Table 2. Hemodynamic Variables in Littermate Control (CTL) and VSMC-Specific ROCK2-Overexpressing (ROCK2-Tg) Mice Under Normoxia and After 4-wk Hypoxia

	Normoxia		Hypoxia	
Parameters	CTL (n=10)	ROCK2-Tg (n=10)	CTL (n=10)	ROCK2-Tg (n=10)
Heat rate, beats/min	528±20	490±16	511±7	510±10
RVSP, mm Hg	28.8±0.7	30.1±0.8	43.6±0.7**	53.9±1.1**††
RVEDP, mm Hg	0.8±0.1	0.9±0.1	1.9±0.3**	3.1±0.2**††
RV dP/dt max, mm Hg/s	3361±185	3250±170	4063±139**	4788±36**††
RV dP/dt min, mm Hg/s	2067±114	1802±111	3221±231**	3999±111**††
Systolic blood pressure, mm Hg	101±2	101±2	103±3	101±3
Diastolic blood pressure, mm Hg	66±2	69±4	66±5	68±2
LVSP, mm Hg	105±4	102±3	108±2	105±2
LVEDP, mm Hg	5.0±0.5	4.9±0.8	5.4±0.6	5.5±0.8
LV dP/dt max, mm Hg/s	10 069±793	9708±742	9947±883	11 008±810
LV dP/dt min, mm Hg/s	7957±547	8474±663	7990±869	8761±783

Results are expressed as mean±SEM. Comparisons were performed using 1-way ANOVA. LV dP/dt max indicates peak rates of LV pressure development; LV dP/dt min, peak rates of LV pressure relaxation; LVEDP, left ventricular end-diastolic pressure; LVSP, left ventricular systolic pressure; ROCK, Rho-kinase; RV dP/dt max, peak rates of RV pressure development; RV dP/dt min, peak rates of RV pressure relaxation; RVEDP, right ventricular end-diastolic pressure; RVSP, right ventricular systolic pressure; and VSMC, vascular smooth muscle cells.

**$P<0.01$ vs normoxia in each group.

††$P<0.01$ vs hypoxic CTL mice.

in IPAH-PASMC was also required for PASMC migration and proliferation. To the best of our knowledge, this is the first study that demonstrates that ROCK2 contributes to the pathogenesis of PAH, suggesting that ROCK2 is an important therapeutic target for the treatment of the disorder.

In the present study, we observed that ROCK2 expression was upregulated in pulmonary arterial media and PASMC from patients with IPAH compared with controls. Interestingly, it has been recently reported that the Rho/ROCK pathway enhances cancer progression and that upregulated ROCK2 levels are observed in esophageal, hepatocellular, colon, and bladder cancer.[22–26] Furthermore, a new concept has recently been proposed that the pathobiology of severe IPAH resembles that of cancers in humans.[27] In the present study, the ROCK2 upregulation in pulmonary arteries from patients with IPAH were associated with enhanced proliferation and migration of PASMC, similar to human cancer cells.

In the present study, we observed that the extent of hypoxia-induced PH was reduced in VSMC-specific ROCK2$^{+/-}$ mice and was enhanced in VSMC-specific ROCK2-Tg mice. The *SM22α* promoter used for the generation of these mice is expressed in both VSMC and cardiac myocytes at early embryonic stages and finally becomes restricted to VSMC at late embryonic stages and throughout adulthood.[28] In addition, these mutant mice showed normal postnatal development with normal cardiac function (Tables 1 and 2). Thus, embryonic lethality observed in VSMC-specific ROCK2$^{-/-}$ mice suggests that ROCK2 plays an essential role, especially in the development of blood vessels.

ROCK activation of the lung tissues from mice was observed in hypoxia-induced PH. We and other group have recently demonstrated a direct evidence for ROCK activation in patients with IPAH.[13,29] Recent studies also reported that increased ROCK activity might be a biological marker for cardiovascular disease.[30–32] We observed that ROCK activity of the lung tissues after chronic hypoxia was reduced in ROCK2$^{+/-}$ mice and was increased in ROCK2-Tg mice compared with respective littermates. Furthermore, similar results were obtained for ERK activity that is known to be important for VSMC migration and proliferation.[33–35] However, we observed less dramatic changes in ROCK and ERK activities compared with those in the degree of PH, which could be explained by the fact that we used whole mouse lung tissue for Western blot that contains not only VSMC but also many other types of cells. In addition, we confirmed that pulmonary arteries from patients with IPAH revealed enhanced ERK activity. Taken together, these results provide the first evidence that ROCK2 in VSMC mediates hypoxia-induced PH in mice through ROCK activation and partially through ERK activation.

We further examined the role of ROCK2 in the VSMC from each genotype of mice and human IPAH-PASMC in vitro. We found that both migration and proliferation were reduced in VSMC from ROCK2$^{+/-}$ mice, as well as in human IPAH-PASMC transfected with *ROCK2*-siRNA. Furthermore, migration was enhanced in VSMC from ROCK2-Tg mice. As described above, ROCK2 overexpression was also observed in IPAH-PASMC, which has been reported to show phenotypically greater migration and proliferation than non-PAH-PASMC.[36,37] Consistently, the expressions of NADPH oxidases (eg, NOX2 and NOX4), which contribute to the pathogenesis of PH,[38,39] were significantly less in ROCK2$^{+/-}$ VSMC and were enhanced in ROCK2-Tg VSMC. In contrast, the expression of HO-1 was significantly increased in ROCK2$^{+/-}$ VSMC and less in ROCK2-Tg VSMC, which is supported by the observation that HO-1 ameliorated hypoxia-induced PH in mice.[40] Importantly, the expression of vascular cell adhesion molecule-1, which contributes to inflammatory cell migration,[20] was significantly less in ROCK2$^{+/-}$ VSMC and increased in ROCK2-Tg VSMC. In addition, ROCK2$^{+/-}$ VSMC secreted less inflammatory cytokines (eg, interferon-γ and tumor necrosis factor-α).[20,21] In contrast, the secretion of these inflammatory cytokines was significantly increased in ROCK2-Tg VSMC. Taken together, we demonstrated that ROCK2 in VSMC may contribute to oxidative stress induction, resulting in VSMC proliferation, adhesion molecule expression, and inflammatory cytokines secretion (Figure X in the online-only Data Supplement). We observed significant increase in the number of CD45-positive inflammatory cells in the lung tissue, which was significantly less in ROCK2$^{+/-}$ mice and was significantly increased in ROCK2-Tg mice compared with the respective littermates (Figures 2E, 2F, 3E, 3F, 4A, 4B, 4G, and 4H).

The secretion of inflammatory cytokines/chemokines and growth factors is regulated by oxidative stress in VSMC.[38] Hypoxia is thought to induce oxidative stress,[41] thereby

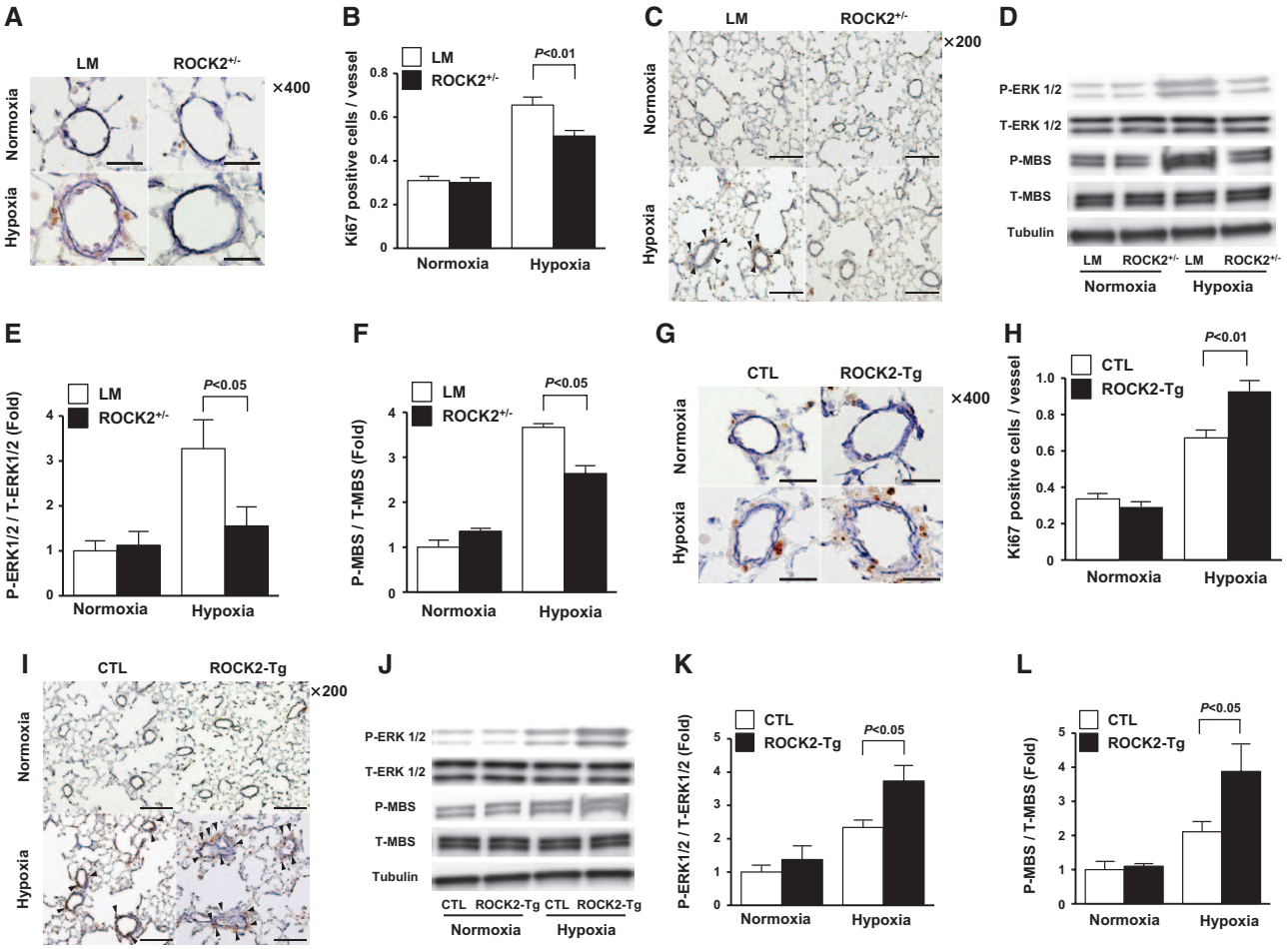

Figure 4. Rho-kinase 2 (ROCK2) in vascular smooth muscle cells (VSMC) modulates pulmonary vascular cell proliferation after chronic hypoxia. VSMC-specific heterozygous ROCK2-deficient mice (ROCK2$^{+/-}$) and littermate control mice (LM; **A**–**F**) and VSMC-specific ROCK2-overexpressing transgenic mice (ROCK2-Tg) and wild-type littermate control mice (CTL; **G**–**L**) were exposed to room air (normoxia) or 10% oxygen (hypoxia) for 4 weeks. **A** and **G**, Representative serial sections of pulmonary arterioles immunostained with antibodies to Ki67. Scale bars=25 μm. **B** and **H**, The number of Ki67-positive inflammatory cells per pulmonary arterioles (n=5 each). **C** and **I**, Representative serial sections of pulmonary arterioles immunostained with antibodies to phosphorylation of ERK 1/2 (P-ERK 1/2). Arrowheads show P-ERK 1/2–positive cells, mainly located in the remodeled pulmonary arterioles after chronic hypoxia. Scale bars=25 μm. **D** and **J**, Representative immunoblots of extracellular signal–regulated kinase (ERK) activity assessed by the ratio of phosphorylated form of ERK 1/2 to total ERK 1/2 (P-ERK 1/2/T-ERK 1/2) and ROCK activity assessed by the ratio of phosphorylated form of the myosin-binding subunit (MBS) at Thr696 to total MBS (P-MBS/T-MBS) in the lung tissues from each experimental group. **E** and **K**, Change of ERK activity quantified by densitometry analysis (n=6 each). **F** and **L**, Change of ROCK activity quantified by densitometry analysis (n=6 each). Results are expressed as mean±SEM.

promoting VSMC proliferation, pulmonary vascular remodeling, and PH.[39,42] Thus, the cooperative interaction between extracellular inflammatory cytokines and pulmonary vascular ROCK2 is critical for the process of hypoxia-induced PH. Therefore, these data support the idea that ROCK2 in VSMC may play a crucial role in the oxidative stress induction, VSMC proliferation, and the development of hypoxia-induced PH.

Besides these results, it has been reported that the inhibition of ROCK2, rather than that of ROCK1, increased apoptosis and decreased contraction in VSMC, ameliorating vascular remodeling in PH.[16,43] Pulmonary arterial endothelial dysfunction, as well as abnormal PASMC phenotype, contributes to the development of PAH.[3] We have previously reported that endothelium-dependent relaxation was significantly impaired in small pulmonary arteries isolated from patients with IPAH compared with controls.[13] Interestingly, it has recently been reported that ROCK2, rather than ROCK1, in endothelial cells contributed to angiogenesis and production of cell adhesion molecules, both of which are known to deteriorate PAH.[44,45] All these observations indicate that ROCK2, rather than ROCK1, is a key regulator of multiple vascular cell functions, especially in VSMC, and could be an important therapeutic target of PAH.

The present findings confirm the importance of ROCK2 of PASMC in the pathogenesis of hypoxia-induced PAH both in vitro and in vivo. However, in some experimental models of PH, ROCK1 may also contribute to the development of PH. In fawn-hooded rats that develop severe PH even under mild hypoxia, ROCK1 expression of pulmonary arteries was increased and fasudil reduced the development of PH.[46] In monocrotaline-injected pneumonectomized rats that develop severe PH, ROCK1 expression of lung tissues was constitutively activated with ROCK activation.[47] In the present study, we also found that migration, but not proliferation, was reduced in IPAH-PASMC transfected with *ROCK1*-siRNA and was further suppressed with dual *ROCK1/2*-siRNA. Thus,

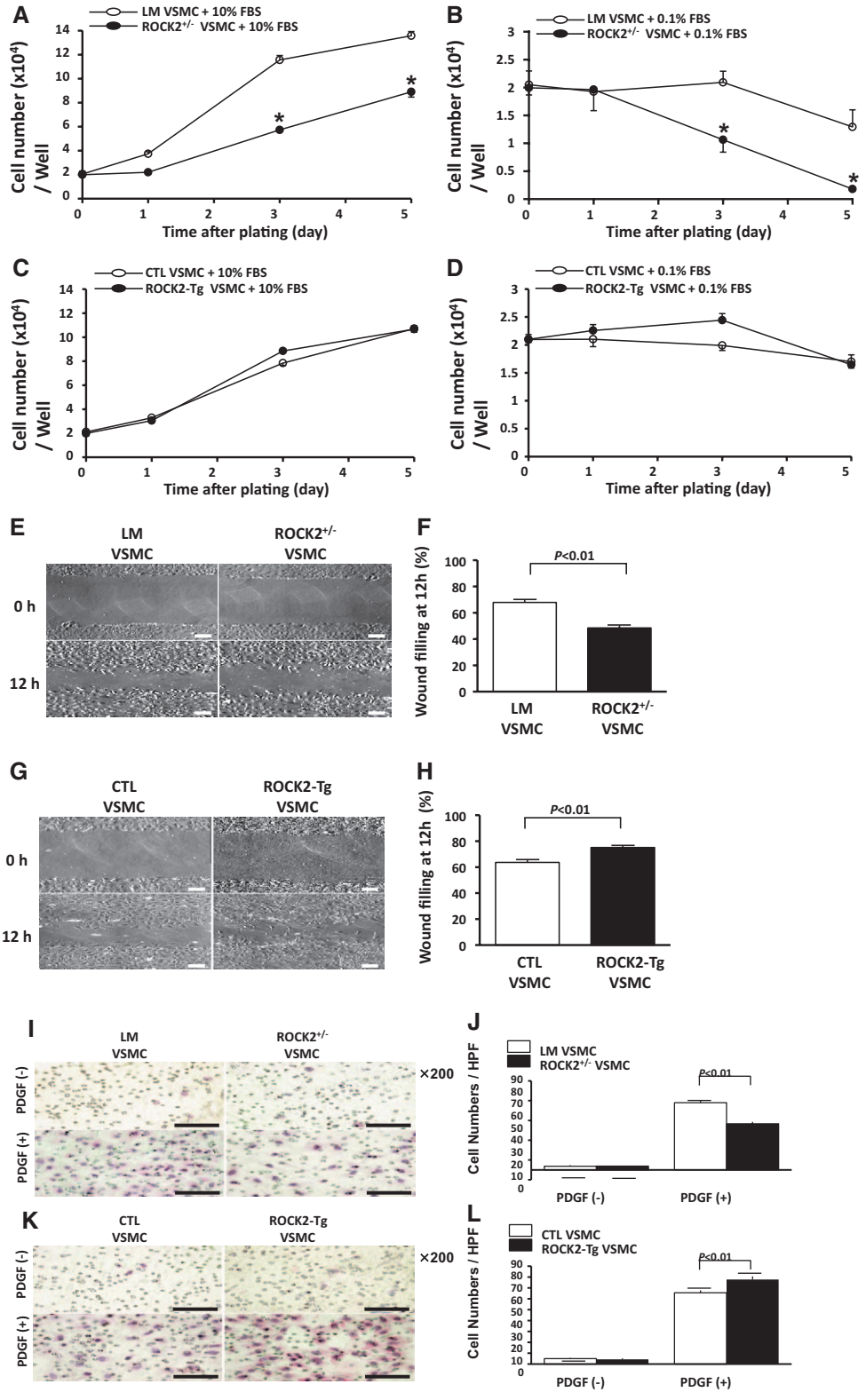

Figure 5. Rho-kinase 2 (ROCK2) mediates vascular smooth muscle cells (VSMC) proliferation and migration in mice in vitro. **A**–**D**, Cell proliferation curve in response to 10% fetal bovine serum (FBS) or 0.1% FBS in VSMC cultured from VSMC-specific heterozygous ROCK2-deficient mice (ROCK2$^{+/-}$ VSMC), littermate control mice (LM VSMC), VSMC-specific ROCK2-overexpressing transgenic mice (ROCK2-Tg VSMC), and wild-type littermate control mice (CTL VSMC; n=9 each). *P<0.01 compared with littermate controls. **E** and **G**, Representative phase-contrast images of scratch assay to analyze VSMC migration in response to 0.1% FBS for 12 h. A cell-free zone of ≈600 μm in width was created by a pipette tip scratch. Scale bars=100 μm. **F** and **H**, Quantitative analysis of scratch assay assessed by the percentage of wound area recovered after 12 h (n=9 each). **I** and **K**, Representative high-power fields (×200 magnification) of a modified Boyden chamber assay to analyze cell migration in response to platelet-derived growth factor (PDGF; 10 ng/mL) for 6 h. VSMC were migrated toward underside of membrane and were stained with hematoxylin and eosin. Scale bars=100 μm. **J** and **L**, The number of VSMC migrated on underside of membrane per high-power fields (HPF) (×400 magnification; n=6 each). Results are expressed as mean±SEM.

ROCK1 might be involved, at least in part, in the pathogenesis of PAH through enhanced PASMC migration.

Several limitations should be mentioned for the present study. First, both ROCK2$^{+/-}$ and ROCK2-Tg mice survived normally under normoxic conditions. It was previously shown that systemic homozygous ROCK2-deficient mice backcrossed into a C57BL/6 background have a low survival rate of <1%.[48] Thus, further studies are needed to determine whether ROCK2 abnormalities affect long-term survival. Second, no systemic or pulmonary hemodynamic abnormalities were noted in ROCK2$^{+/-}$ mice under basal normoxic conditions. ROCK2, rather than ROCK1, seems to be essential for the regulation

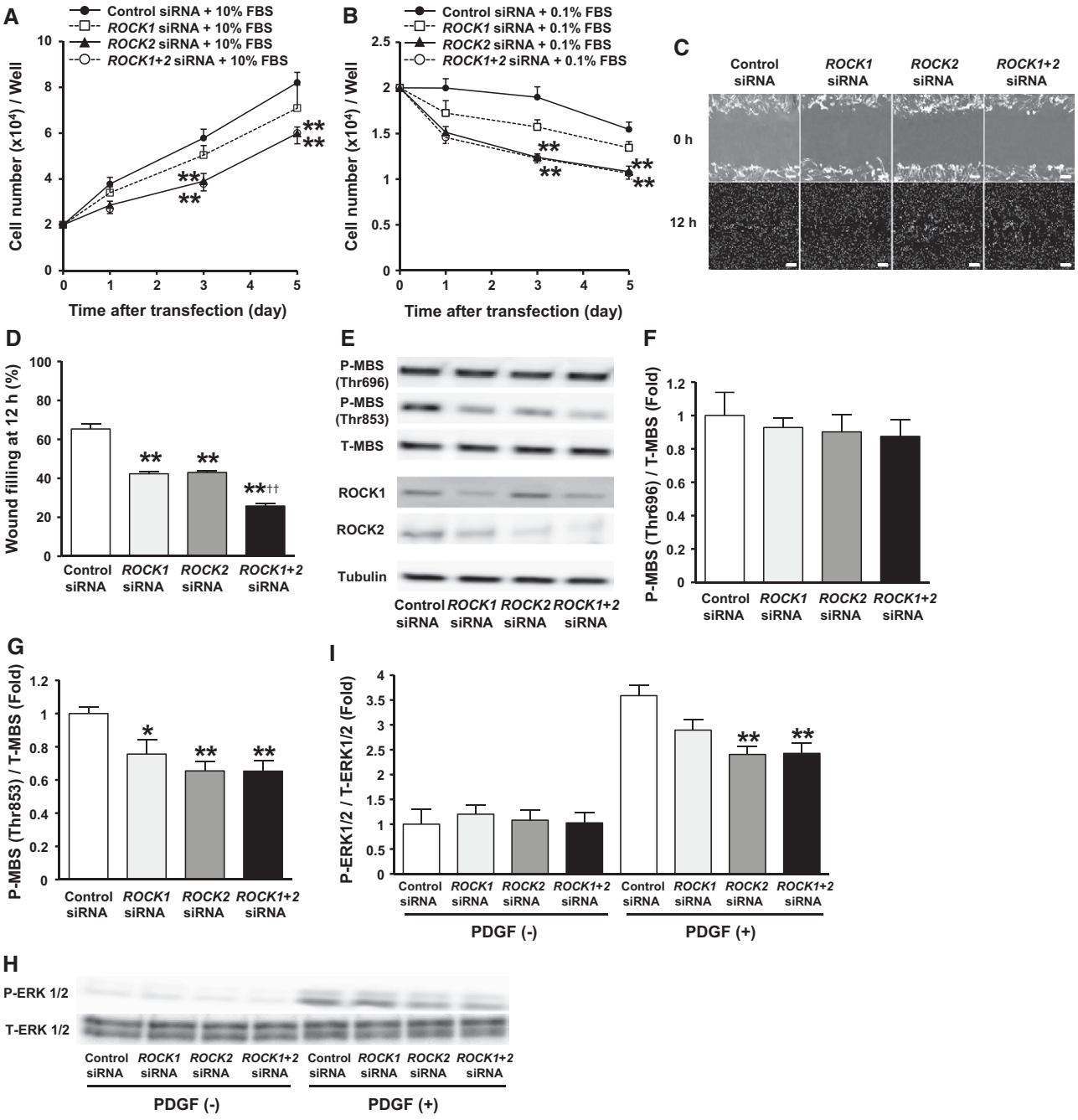

Figure 6. Rho-kinase 2 (ROCK2) mediates proliferation and migration of pulmonary arterial smooth muscle cells (PASMC) from a patient with idiopathic pulmonary arterial hypertension (IPAH; IPAH-PASMC). **A** and **B**, Cell proliferation curve in response to 10% fetal bovine serum (FBS) or 0.1% FBS in IPAH-PASMC after transfection with 30 nmol/L control, *ROCK1*-, *ROCK2*-, or dual *ROCK1/2*-small interfering RNA (siRNA; n=12 each). **C**, Representative phase-contrast images of scratch assay to analyze cell migration in response to 0.1% FBS for 12 h in IPAH-PASMC transfected with each siRNA (30 nmol/L). A cell-free zone of ≈600 μm in width was created by a pipette tip scratch. Scale bars=100 μm. **D**, Quantitative analysis of scratch assay assessed by the percentage of wound area recovered after 12 h (n=9 each). **E**, Representative immunoblots of phosphorylation of the myosin-binding subunit (MBS) at Thr696 or Thr853 (P-MBS) and total MBS (T-MBS) in IPAH-PSMC transfected with each siRNA (30 nmol/L) in normal medium containing 10% FBS. **F** and **G**, Densitometry analysis of ROCK activity assessed by the ratio of P-MBS at Thr696 or Thr853 to T-MBS (P-MBS/T-MBS) in IPAH-PSMC transfected with each siRNA (n=4 each). **H**, Representative immunoblots of phosphorylation of extracellular signal–regulated kinase 1/2 (P-ERK 1/2) and total ERK 1/2 (T-ERK 1/2) in response to platelet-derived growth factor (PDGF; 10 ng/mL) for 10 minutes in IPAH-PSMC transfected with each siRNA (30nM). **I**, Densitometry analysis of ERK activity as assessed by the ratio of P-ERK 1/2 to T-ERK 1/2 (P-ERK1/2/T-ERK1/2) in IPAH-PSMC transfected with each siRNA (n=4 each). **P*<0.05, ***P*<0.01 compared with control siRNA, and ††*P*<0.01 compared with ROCK1- or ROCK2-siRNA. Results are expressed as mean±SEM.

of arterial pressure because systemic heterozygous ROCK1-deficient mice have normal basal blood pressure.[49] It is conceivable that in the present study, only a 24% reduction in ROCK2 protein expression in aortic VSMC may have no significant hemodynamic effects in ROCK2$^{+/-}$ mice. Third, in the present study, we used mouse aortic VSMC, but not PASMC, because of technical reasons, although it is well-known that the effects of hypoxia on the aorta and systemic vessels have

different features from those on the pulmonary circulation. Instead of using mouse PASMC, we performed mechanistic analyses using PASMC from a patient with IPAH. However, because both cultured VSMC and PASMC change their phenotype during passage, our results obtained in vitro might not directly reflect the in vivo results. Fourth, we were unable to adjust the extent of ROCK2 overexpression in mice with that of patients with IPAH. However, the extent of ROCK2 mRNA upregulation in human IPAH-PASMC (1.8-fold increase) was fairly comparable with that in VSMC from ROCK2-Tg mice (1.4-fold increase). Thus, we think that the present results have important clinical implications to better understand the role of ROCK2 in the pathogenesis of PAH. Fifth, although we conventionally evaluated VSMC proliferation using cell count analysis, other additional cell proliferation or apoptosis assays had better be performed. Instead, we assessed ROCK2-induced oxidative stress and secretions of inflammatory cytokines, which contribute to VSMC proliferation.

The present study has important clinical implications. We have previously reported that an isoform-nonspecific ROCK inhibitor, fasudil, abolishes increased vasoconstriction of pulmonary arteries from patients with IPAH.[13] We also have demonstrated that fasudil exerts acute and effective pulmonary vasodilator responses in patients with severe PAH.[50,51] Furthermore, the present findings suggest that the beneficial effects of fasudil are mediated mainly by its suppression of ROCK2 with a resultant inhibition of PASMC proliferation and migration. Thus, we have started the clinical trial with an oral form of long-acting fasudil for the long-term treatment of patients with PAH to evaluate its effect on pulmonary hemodynamics and prognosis. In summary, the present study provides the first evidence that ROCK2 in VSMC contributes to the pathogenesis of PAH.

Acknowledgments

We thank Drs Nakamura and Ito, Department of Cardiovascular Medicine, Okayama University Graduate School of Medicine, Dentistry and Pharmaceutical Sciences, for providing the 2 lines of IPAH-PASMC used in the present study. We also thank A. Saito, T. Hiroi, and Y. Watanabe for excellent technical assistance.

Sources of Funding

This work was supported, in part, by the Grant-in-Aid for Scientific Research on Innovative Areas, the Grant-in-Aid for Tohoku University Global COE for Conquest of Signal Transduction Diseases with Network Medicine, and the Grants-in-Aid for Scientific Research, all of which are from the Ministry of Education, Culture, Sports, Science, and Technology, Tokyo, Japan.

Disclosures

None.

References

1. Humbert M, Sitbon O, Chaouat A, et al. Survival in patients with idiopathic, familial, and anorexigen-associated pulmonary arterial hypertension in the modern management era. *Circulation*. 2010;122:156–163.
2. Fukumoto Y, Shimokawa H. Recent progress in the management of pulmonary hypertension. *Circ J*. 2011;75:1801–1810.
3. Morrell NW, Adnot S, Archer SL, Dupuis J, Jones PL, MacLean MR, McMurtry IF, Stenmark KR, Thistlethwaite PA, Weissmann N, Yuan JX, Weir EK. Cellular and molecular basis of pulmonary arterial hypertension. *J Am Coll Cardiol*. 2009;54(1 suppl):S20–S31.
4. Shimokawa H, Rashid M. Development of Rho-kinase inhibitors for cardiovascular medicine. *Trends Pharmacol Sci*. 2007;28:296–302.
5. Satoh K, Fukumoto Y, Shimokawa H. Rho-kinase: important new therapeutic target in cardiovascular diseases. *Am J Physiol Heart Circ Physiol*. 2011;301:H287–H296.
6. Nakagawa O, Fujisawa K, Ishizaki T, Saito Y, Nakao K, Narumiya S. ROCK-I and ROCK-II, two isoforms of Rho-associated coiled-coil forming protein serine/threonine kinase in mice. *FEBS Lett*. 1996;392:189–193.
7. Chevrier V, Piel M, Collomb N, Saoudi Y, Frank R, Paintrand M, Narumiya S, Bornens M, Job D. The Rho-associated protein kinase p160ROCK is required for centrosome positioning. *J Cell Biol*. 2002;157:807–817.
8. Wei L, Roberts W, Wang L, Yamada M, Zhang S, Zhao Z, Rivkees SA, Schwartz RJ, Imanaka-Yoshida K. Rho kinases play an obligatory role in vertebrate embryonic organogenesis. *Development*. 2001;128:2953–2962.
9. Shimizu Y, Thumkeo D, Keel J, Ishizaki T, Oshima H, Oshima M, Noda Y, Matsumura F, Taketo MM, Narumiya S. ROCK-I regulates closure of the eyelids and ventral body wall by inducing assembly of actomyosin bundles. *J Cell Biol*. 2005;168:941–953.
10. Thumkeo D, Keel J, Ishizaki T, Hirose M, Nonomura K, Oshima H, Oshima M, Taketo MM, Narumiya S. Targeted disruption of the mouse rho-associated kinase 2 gene results in intrauterine growth retardation and fetal death. *Mol Cell Biol*. 2003;23:5043–5055.
11. Abe K, Tawara S, Oi K, Hizume T, Uwatoku T, Fukumoto Y, Kaibuchi K, Shimokawa H. Long-term inhibition of Rho-kinase ameliorates hypoxia-induced pulmonary hypertension in mice. *J Cardiovasc Pharmacol*. 2006;48:280–285.
12. Abe K, Shimokawa H, Morikawa K, Uwatoku T, Oi K, Matsumoto Y, Hattori T, Nakashima Y, Kaibuchi K, Sueishi K, Takeshit A. Long-term treatment with a Rho-kinase inhibitor improves monocrotaline-induced fatal pulmonary hypertension in rats. *Circ Res*. 2004;94:385–393.
13. Do e Z, Fukumoto Y, Takaki A, Tawara S, Ohashi J, Nakano M, Tada T, Saji K, Sugimura K, Fujita H, Hoshikawa Y, Nawata J, Kondo T, Shimokawa H. Evidence for Rho-kinase activation in patients with pulmonary arterial hypertension. *Circ J*. 2009;73:1731–1739.
14. Oka M, Fagan KA, Jones PL, McMurtry IF. Therapeutic potential of RhoA/Rho kinase inhibitors in pulmonary hypertension. *Br J Pharmacol*. 2008;155:444–454.
15. Noma K, Rikitake Y, Oyama N, Yan G, Alcaide P, Liu PY, Wang H, Ahl D, Sawada N, Okamoto R, Hiroi Y, Shimizu K, Luscinskas FW, Sun J, Liao JK. ROCK1 mediates leukocyte recruitment and neointima formation following vascular injury. *J Clin Invest*. 2008;118:1632–1644.
16. Wang Y, Zheng XR, Riddick N, Bryden M, Baur W, Zhang X, Surks HK. ROCK isoform regulation of myosin phosphatase and contractility in vascular smooth muscle cells. *Circ Res*. 2009;104:531–540.
17. Rabinovitch M, Gamble W, Nadas AS, Miettinen OS, Reid L. Rat pulmonary circulation after chronic hypoxia: hemodynamic and structural features. *Am J Physiol*. 1979;236:H818–H827.
18. Rabinovitch M. Molecular pathogenesis of pulmonary arterial hypertension. *J Clin Invest*. 2012;122:4306–4313.
19. Cheng C, Haasdijk RA, Tempel D, den Dekker WK, Chrifi I, Blonden LA, van de Kamp EH, de Boer M, Bürgisser PE, Noorderloos A, Rens JA, ten Hagen TL, Duckers HJ. PDGF-induced migration of vascular smooth muscle cells is inhibited by heme oxygenase-1 via VEGFR2 upregulation and subsequent assembly of inactive VEGFR2/PDGFRβ heterodimers. *Arterioscler Thromb Vasc Biol*. 2012;32:1289–1298.
20. Doran AC, Meller N, McNamara CA. Role of smooth muscle cells in the initiation and early progression of atherosclerosis. *Arterioscler Thromb Vasc Biol*. 2008;28:812–819.
21. Jovinge S, Hultgårdh-Nilsson A, Regnström J, Nilsson J. Tumor necrosis factor-alpha activates smooth muscle cell migration in culture and is expressed in the balloon-injured rat aorta. *Arterioscler Thromb Vasc Biol*. 1997;17:490–497.
22. Narumiya S, Tanji M, Ishizaki T. Rho signaling, ROCK and mDia1, in transformation, metastasis and invasion. *Cancer Metastasis Rev*. 2009;28:65–76.
23. Yibulayin W, Chen ZL, Tan FW, Sun N, He J. Relationship between ROCK2 expression and clinicopathologic characteristics of esophageal squamous cell carcinoma. *Zhonghua Yi Xue Za Zhi*. 2011;91:2038–2041.
24. Wong CC, Wong CM, Tung EK, Man K, Ng IO. Rho-kinase 2 is frequently overexpressed in hepatocellular carcinoma and involved in tumor invasion. *Hepatology*. 2009;49:1583–1594.
25. Vishnubhotla R, Sun S, Huq J, Bulic M, Ramesh A, Guzman G, Cho M, Glover SC. ROCK-II mediates colon cancer invasion via regulation of MMP-2 and MMP-13 at the site of invadopodia as revealed by multiphoton imaging. *Lab Invest*. 2007;87:1149–1158.

26. Kamai T, Tsujii T, Arai K, Takagi K, Asami H, Ito Y, Oshima H. Significant association of Rho/ROCK pathway with invasion and metastasis of bladder cancer. *Clin Cancer Res*. 2003;9:2632–2641.
27. Sakao S, Tatsumi K. Vascular remodeling in pulmonary arterial hypertension: multiple cancer-like pathways and possible treatment modalities. *Int J Cardiol*. 2011;147:4–12.
28. Lepore JJ, Cheng L, Min Lu M, Mericko PA, Morrisey EE, Parmacek MS. High-efficiency somatic mutagenesis in smooth muscle cells and cardiac myocytes in SM22alpha-Cre transgenic mice. *Genesis*. 2005;41:179–184.
29. Guilluy C, Eddahibi S, Agard C, Guignabert C, Izikki M, Tu L, Savale L, Humbert M, Fadel E, Adnot S, Loirand G, Pacaud P. RhoA and Rho kinase activation in human pulmonary hypertension: role of 5-HT signaling. *Am J Respir Crit Care Med*. 2009;179:1151–1158.
30. Soga J, Noma K, Hata T, Hidaka T, Fujii Y, Idei N, Fujimura N, Mikami S, Maruhashi T, Kihara Y, Chayama K, Kato H, Liao JK, Higashi Y; ROCK Study Group. Rho-associated kinase activity, endothelial function, and cardiovascular risk factors. *Arterioscler Thromb Vasc Biol*. 2011;31:2353–2359.
31. Ocaranza MP, Gabrielli L, Mora I, Garcia L, McNab P, Godoy I, Braun S, Córdova S, Castro P, Novoa U, Chiong M, Lavandero S, Jalil JE. Markedly increased Rho-kinase activity in circulating leukocytes in patients with chronic heart failure. *Am Heart J*. 2011;161:931–937.
32. Kikuchi Y, Yasuda S, Aizawa K, Tsuburaya R, Ito Y, Takeda M, Nakayama M, Ito K, Takahashi J, Shimokawa H. Enhanced Rho-kinase activity in circulating neutrophils of patients with vasospastic angina: a possible biomarker for diagnosis and disease activity assessment. *J Am Coll Cardiol*. 2011;58:1231–1237.
33. Ai S, Kuzuya M, Koike T, Asai T, Kanda S, Maeda K, Shibata T, Iguchi A. Rho-Rho kinase is involved in smooth muscle cell migration through myosin light chain phosphorylation-dependent and independent pathways. *Atherosclerosis*. 2001;155:321–327.
34. Zhan Y, Kim S, Izumi Y, Izumiya Y, Nakao T, Miyazaki H, Iwao H. Role of JNK, p38, and ERK in platelet-derived growth factor-induced vascular proliferation, migration, and gene expression. *Arterioscler Thromb Vasc Biol*. 2003;23:795–801.
35. Kamiyama M, Utsunomiya K, Taniguchi K, Yokota T, Kurata H, Tajima N, Kondo K. Contribution of Rho A and Rho kinase to platelet-derived growth factor-BB-induced proliferation of vascular smooth muscle cells. *J Atheroscler Thromb*. 2003;10:117–123.
36. Sanchez O, Marcos E, Perros F, Fadel E, Tu L, Humbert M, Dartevelle P, Simonneau G, Adnot S, Eddahibi S. Role of endothelium-derived CC chemokine ligand 2 in idiopathic pulmonary arterial hypertension. *Am J Respir Crit Care Med*. 2007;176:1041–1047.
37. Ogawa A, Nakamura K, Matsubara H, Fujio H, Ikeda T, Kobayashi K, Miyazaki I, Asanuma M, Miyaji K, Miura D, Kusano KF, Date H, Ohe T. Prednisolone inhibits proliferation of cultured pulmonary artery smooth muscle cells of patients with idiopathic pulmonary arterial hypertension. *Circulation*. 2005;112:1806–1812.
38. Mittal M, Roth M, König P, et al. Hypoxia-dependent regulation of nonphagocytic NADPH oxidase subunit NOX4 in the pulmonary vasculature. *Circ Res*. 2007;101:258–267.
39. Liu JQ, Zelko IN, Erbynn EM, Sham JS, Folz RJ. Hypoxic pulmonary hypertension: role of superoxide and NADPH oxidase (gp91phox). *Am J Physiol Lung Cell Mol Physiol*. 2006;290:L2–10.
40. Minamino T, Christou H, Hsieh CM, Liu Y, Dhawan V, Abraham NG, Perrella MA, Mitsialis SA, Kourembanas S. Targeted expression of heme oxygenase-1 prevents the pulmonary inflammatory and vascular responses to hypoxia. *Proc Natl Acad Sci U S A*. 2001;98:8798–8803.
41. Sanders KA, Hoidal JR. The NOX on pulmonary hypertension. *Circ Res*. 2007;101:224–226.
42. Stenmark KR, Fagan KA, Frid MG. Hypoxia-induced pulmonary vascular remodeling: cellular and molecular mechanisms. *Circ Res*. 2006;99:675–691.
43. Xu EZ, Kantores C, Ivanovska J, Engelberts D, Kavanagh BP, McNamara PJ, Jankov RP. Rescue treatment with a Rho-kinase inhibitor normalizes right ventricular function and reverses remodeling in juvenile rats with chronic pulmonary hypertension. *Am J Physiol Heart Circ Physiol*. 2010;299:H1854–H1864.
44. Shimada H, Rajagopalan LE. Rho kinase-2 activation in human endothelial cells drives lysophosphatidic acid-mediated expression of cell adhesion molecules via NF-kappaB p65. *J Biol Chem*. 2010;285:12536–12542.
45. Bryan BA, Dennstedt E, Mitchell DC, Walshe TE, Noma K, Loureiro R, Saint-Geniez M, Campaigniac JP, Liao JK, D'Amore PA. RhoA/ROCK signaling is essential for multiple aspects of VEGF-mediated angiogenesis. *FASEB J*. 2010;24:3186–3195.
46. Nagaoka T, Gebb SA, Karoor V, Homma N, Morris KG, McMurtry IF, Oka M. Involvement of RhoA/Rho kinase signaling in pulmonary hypertension of the fawn-hooded rat. *J Appl Physiol (1985)*. 2006;100:996–1002.
47. Homma N, Nagaoka T, Karoor V, Imamura M, Taraseviciene-Stewart L, Walker LA, Fagan KA, McMurtry IF, Oka M. Involvement of RhoA/Rho kinase signaling in protection against monocrotaline-induced pulmonary hypertension in pneumonectomized rats by dehydroepiandrosterone. *Am J Physiol Lung Cell Mol Physiol*. 2008;295:L71–L78.
48. Thumkeo D, Shimizu Y, Sakamoto S, Yamada S, Narumiya S. ROCK-I and ROCK-II cooperatively regulate closure of eyelid and ventral body wall in mouse embryo. *Genes Cells*. 2005;10:825–834.
49. Rikitake Y, Oyama N, Wang CY, Noma K, Satoh M, Kim HH, Liao JK. Decreased perivascular fibrosis but not cardiac hypertrophy in ROCK1+/- haploinsufficient mice. *Circulation*. 2005;112:2959–2965.
50. Fujita H, Fukumoto Y, Saji K, Sugimura K, Demachi J, Nawata J, Shimokawa H. Acute vasodilator effects of inhaled fasudil, a specific Rho-kinase inhibitor, in patients with pulmonary arterial hypertension. *Heart Vessels*. 2010;25:144–149.
51. Fukumoto Y, Matoba T, Ito A, Tanaka H, Kishi T, Hayashidani S, Abe K, Takeshita A, Shimokawa H. Acute vasodilator effects of a Rho-kinase inhibitor, fasudil, in patients with severe pulmonary hypertension. *Heart*. 2005;91:391–392.

Significance

There is increasing evidence for Rho/Rho-kinase (ROCK) pathway in the pathogenesis of pulmonary arterial hypertension (PAH) by accelerating vasoconstriction, migration, and proliferation of pulmonary arterial vascular smooth muscle cells (PASMC). In addition, isoform-nonspecific ROCK inhibitors seem to be a promising treatment for PAH. However, Rho-kinase has 2 isoforms, ROCK1 for circulating inflammatory cells and ROCK2 for the vasculature, and it remains unknown whether ROCK2 in PASMC is involved in PAH pathogenesis. Here, we show that ROCK2 in PASMC contributes to the development of PAH in cells, animals, and humans compared with ROCK1. Focusing on vascular remodeling, ROCK2 in PASMC affects both cell migration and proliferation through ROCK and ERK activation. These findings suggest that ROCK2 in PASMC plays an important role in PAH pathogenesis and may provide the more effective therapeutic strategy for the treatment of PAH.

Arteriosclerosis, Thrombosis, and Vascular Biology

JOURNAL OF THE AMERICAN HEART ASSOCIATION

Crucial Role of ROCK2 in Vascular Smooth Muscle Cells for Hypoxia-Induced Pulmonary Hypertension in Mice

Toru Shimizu, Yoshihiro Fukumoto, Shin-ichi Tanaka, Kimio Satoh, Shohei Ikeda and Hiroaki Shimokawa

Arterioscler Thromb Vasc Biol. 2013;33:2780-2791; originally published online October 17, 2013;
doi: 10.1161/ATVBAHA.113.301357
Arteriosclerosis, Thrombosis, and Vascular Biology is published by the American Heart Association, 7272 Greenville Avenue, Dallas, TX 75231

Print ISSN: 1079-5642. Online ISSN: 1524-4636

Supplemental Figure I

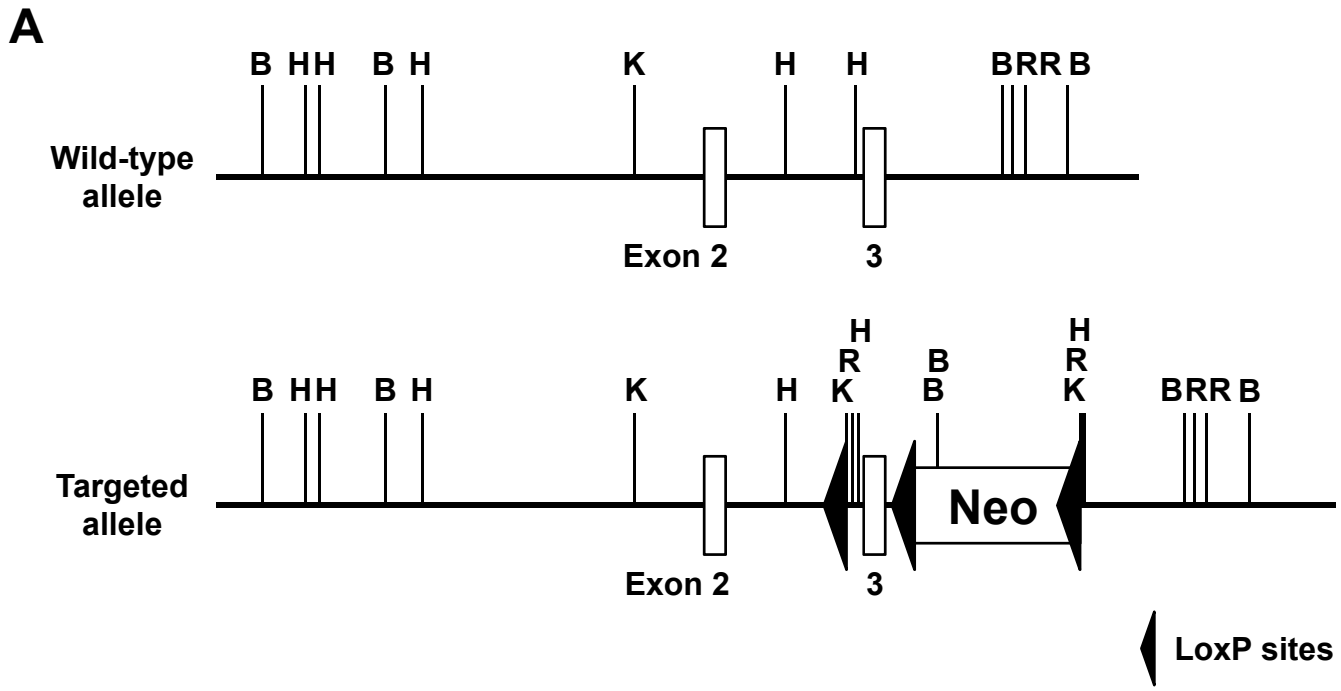

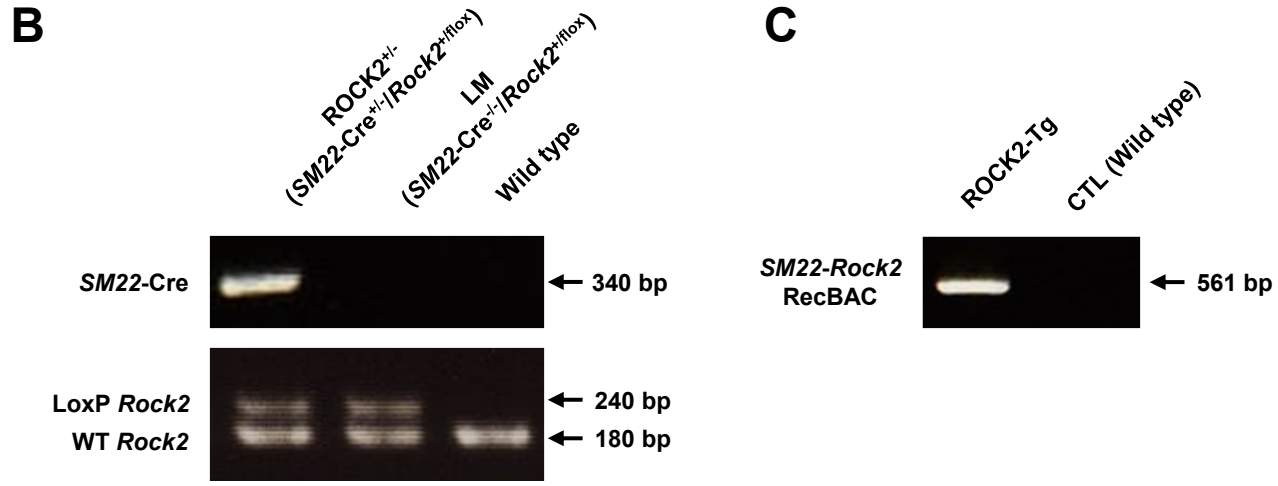

Supplemental Figure I. Generation of *Rock2*-deficient allele and genotyping of VSMC-specific ROCK2-deficient and VSMC-specific ROCK2-overexpressing mouse.
(**A**) Illustration of wild-type *Rock2* allele and conditional targeted allele (floxed allele). *Rock2* exon 3 was removed by the Cre-loxP system to suppress *Rock2* expression. Exon 2 and 3 and loxP sites are indicated as a while box and black arrowheads, respectively. Vertical lines indicate the restriction site; B, *Bgl* II; H, *Hmd* III; K, *Kpn* I; R, *EcoR* I. (**B**) Genotyping by PCR on genomic DNA isolated from the tail of VSMC-specific heterozygous ROCK2-deficient (Rock2$^{+/-}$: *SM22*-Cre$^{+/-}$/*Rock2*$^{+/flox}$), littermate control (LM: *SM22*-Cre$^{-/-}$/*Rock2*$^{+/flox}$), and wild-type mice. The *SM22*-Cre gene, the *Rock2* gene flanked by loxP sites and the wild-type gene were confirmed. (**C**) Genotyping by PCR on genomic DNA isolated from the tail of VSMC-specific ROCK2-overexpressing transgenic (ROCK2-Tg) and wild-type littermate control mice (CTL).

Supplemental Figure II

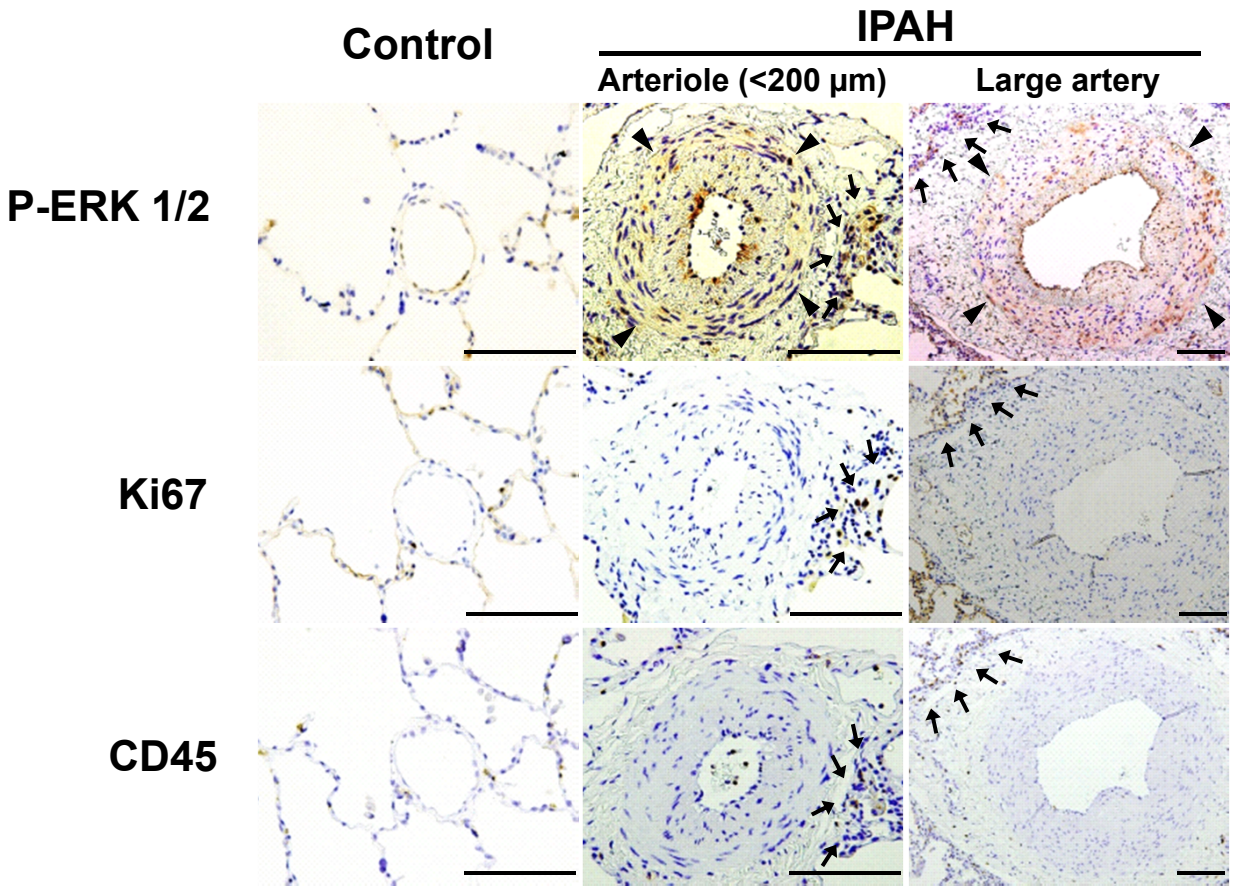

Supplemetal Figure II. Increased number of proliferating and inflammatory cells around the pulmonary arteries from patients with IPAH.
Representative serial lung sections immunostained with antibodies to phosphorylation of extracellular signal-regulated kinase 1/2 (P-ERK 1/2), Ki67, and CD45. **Arrowheads** show strong expression of P-ERK 1/2 in the media of pulmonary arterioles (<200 μm) and large arteries from IPAH patients compared with control patients. **Arrows** show co-expression of P-ERK 1/2-, Ki67-, and CD45-positive cells around pulmonary arterioles and large arteries from IPAH patients. Scale bars=100 μm.

Supplemental Figure III

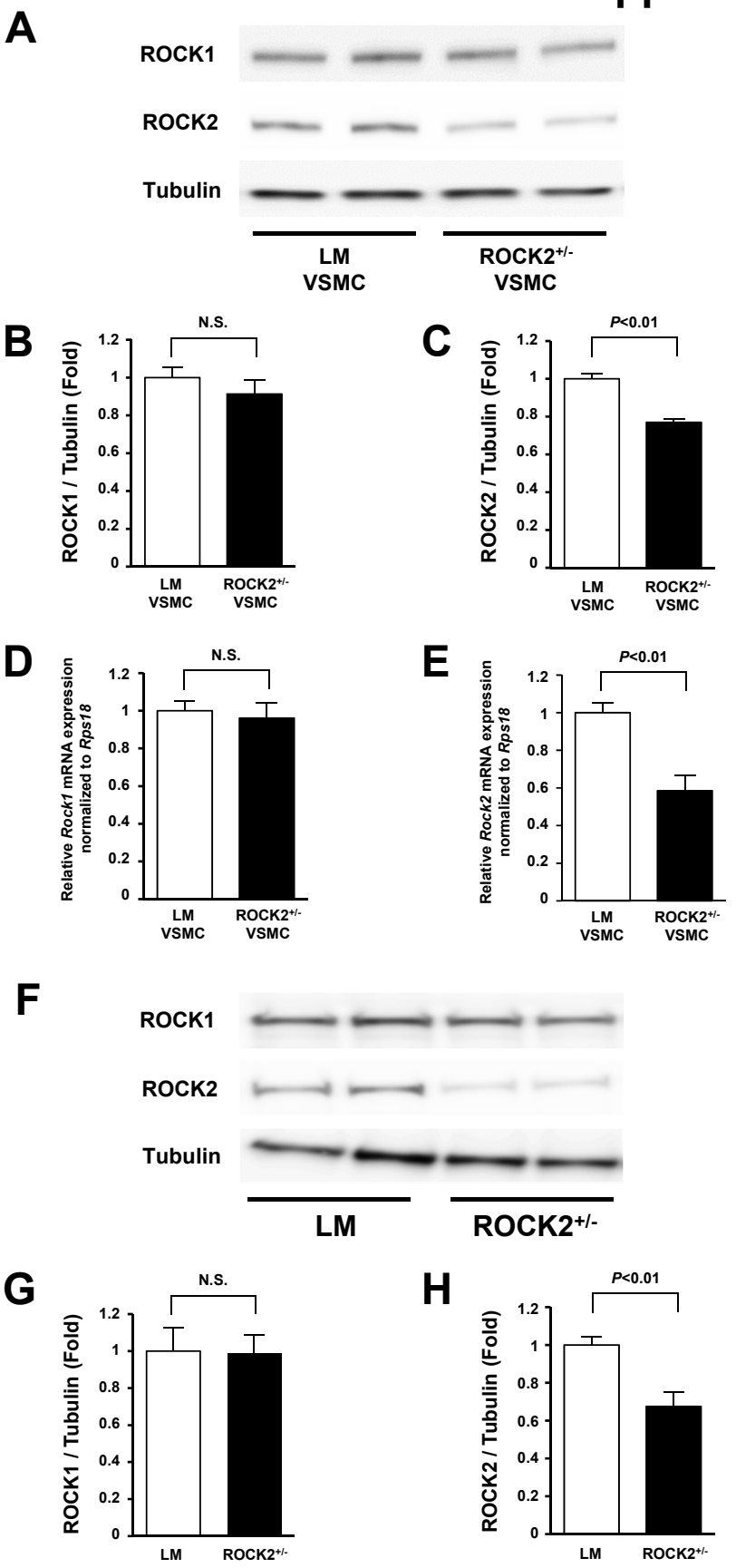

Supplemental Figure III. Reduced ROCK2 expression in VSMC from VSMC-specific heterozygous ROCK2-deficient (ROCK2$^{+/-}$) mice.

(**A**) Representative immunoblots of ROCK1 and ROCK2 in VSMC from ROCK2$^{+/-}$ and littermate control (LM) mice. (**B**, **C**) Quantitative analysis of ROCK1 and ROCK2 protein in VSMC cultured from ROCK2$^{+/-}$ and LM mice (n=4 each). (**D**, **E**) Quantitative analysis of *Rock1* and *Rock2* mRNA in VSMC from ROCK2$^{+/-}$ and LM mice (n=4). (**F**) Representative immunoblots of ROCK1 and ROCK2 in the denuded aorta from ROCK2$^{+/-}$ and LM mice. (**G**, **H**) Quantitative analysis of ROCK1 and ROCK2 protein in the denuded aorta from ROCK2$^{+/-}$ and LM mice (n=4). Results are expressed as mean ± SEM.

Supplemental Figure IV

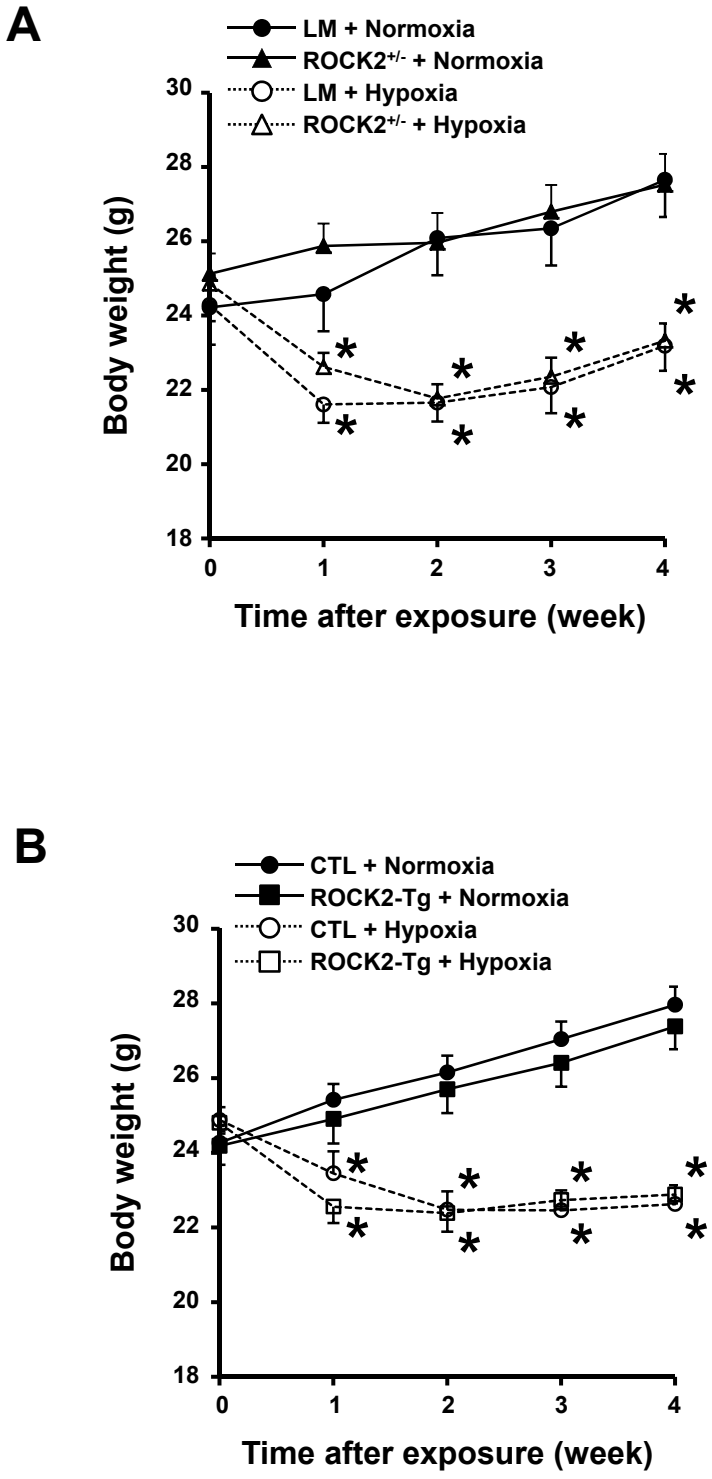

Supplemental Figure IV. Body weight gain for each genotype of mice under normoxic and hypoxic conditions.
(**A**, **B**) Body weight gain during exposure to room air (normoxia) and 10% O_2 (hypoxia) for 4 weeks in VSMC-specific heterozygous ROCK2-deficient mice ($ROCK2^{+/-}$) and littermate control mice (LM), and VSMC-specific ROCK2-overexpressing transgenic mice (ROCK2-Tg) and littermate control mice (CTL) (n=10 each). *P<0.01 compared with respective normoxic counterparts. Results are expressed as mean ± SEM.

Supplemental Figure V

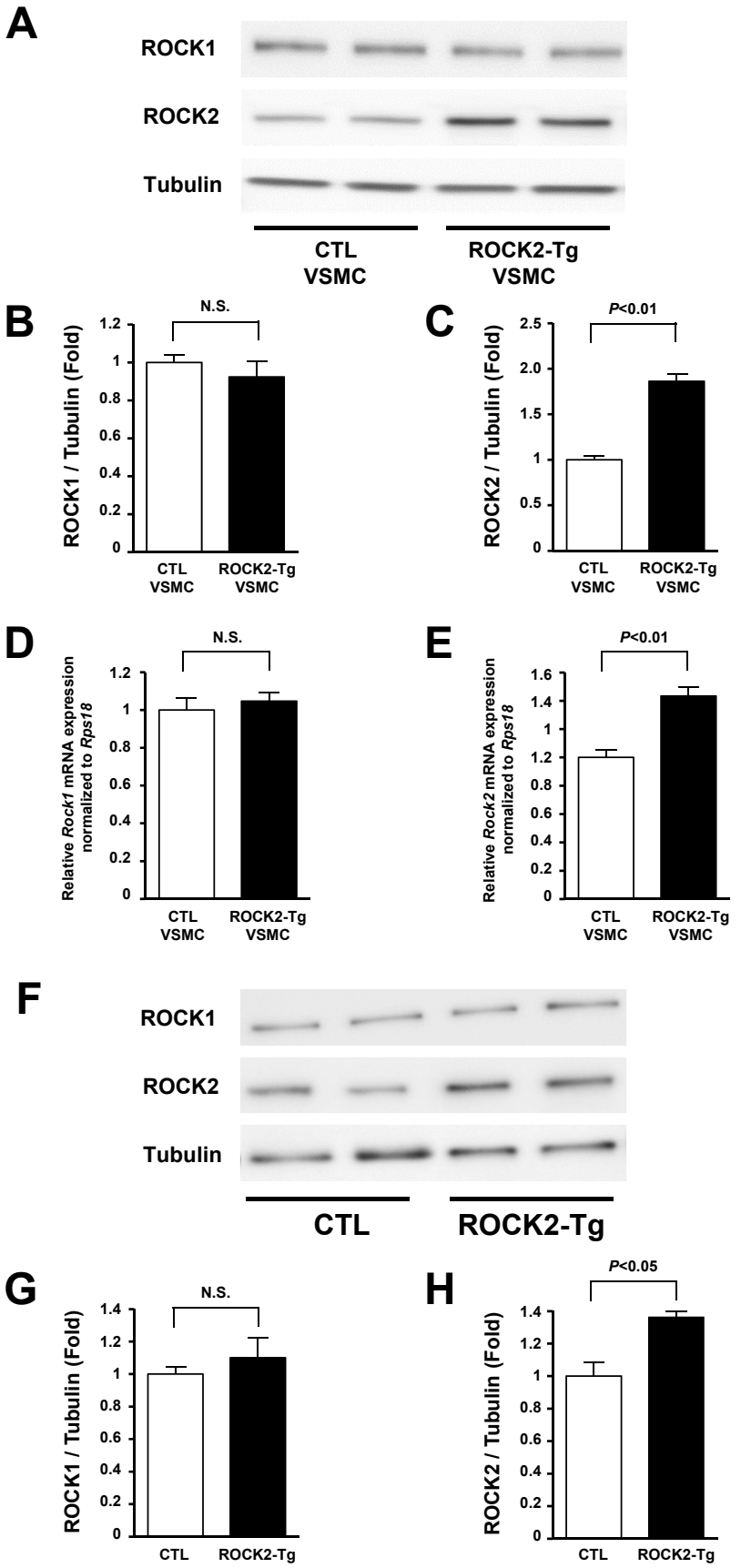

Supplemental Figure V. Increased ROCK2 expression in VSMC and the whole aorta from VSMC-specific ROCK2-overexpressing transgenic (ROCK2-Tg) mice.
(**A**) Representative immunoblots of ROCK1 and ROCK2 in VSMC from ROCK2-Tg and littermate control (CTL) mice. (**B, C**) Quantitative analysis of ROCK1 and ROCK2 protein in VSMC cultured from ROCK2-Tg mice and CTL (n=4 each). (**D, E**) Quantitative analysis of *Rock1* and *Rock2* mRNA in VSMC from ROCK2-Tg and CTL mice (n=4). (**F**) Representative immunoblots of ROCK1 and ROCK2 in the aorta from ROCK2-Tg and CTL mice. (**G, H**) Quantitative analysis of ROCK1 and ROCK2 protein in the whole aorta from ROCK2-Tg and CTL mice (n=4). Results are expressed as mean ± SEM.

Supplemental Figure VI

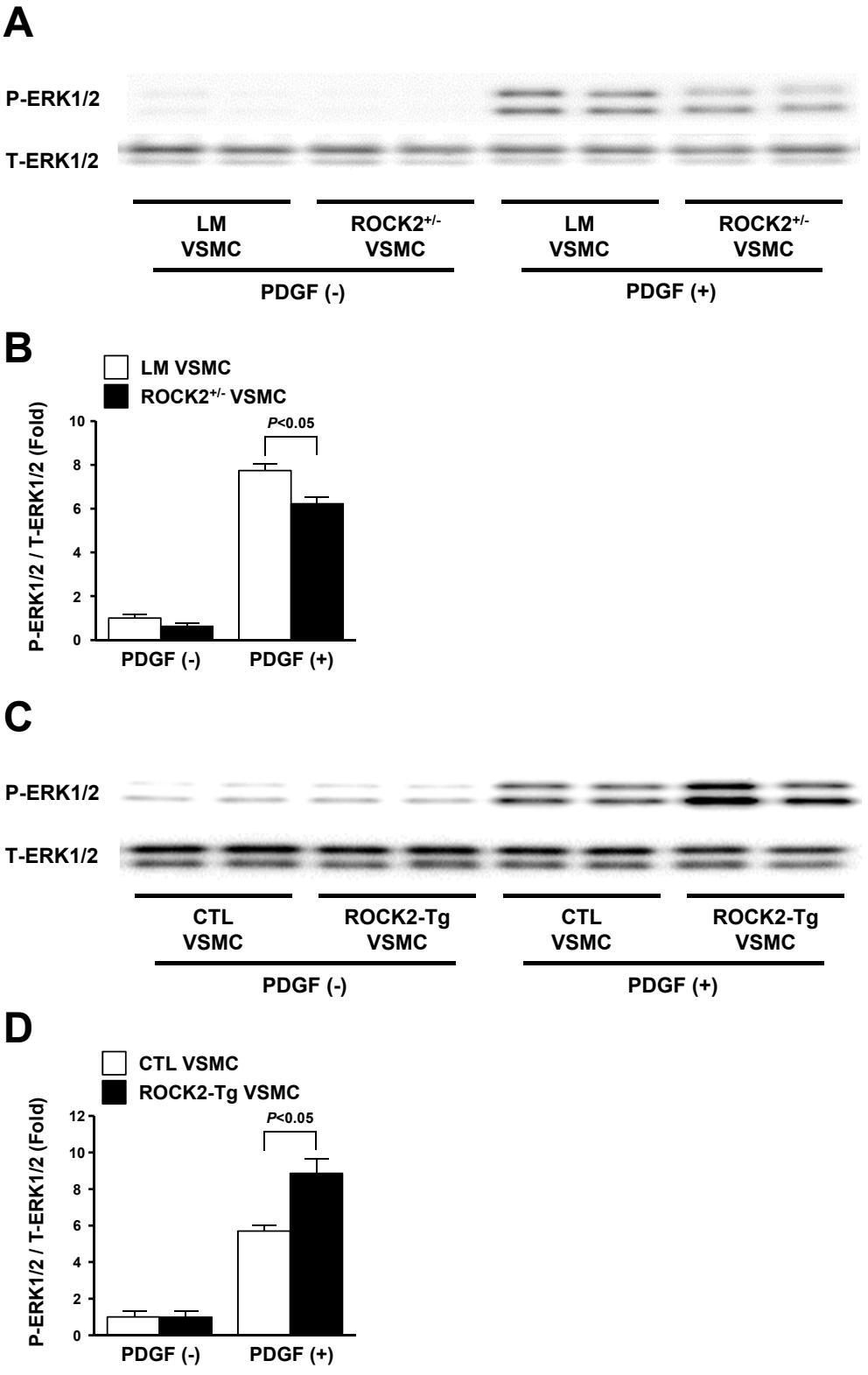

Supplemental Figure VI. ROCK2 mediates ERK activation in response to PDGF stimulation in VSMC in mice in vitro.

(**A**) Representative immunoblots of ERK activity, as assessed by the ratio of phosphorylated ERK1/2 to total ERK 1/2 (P-ERK1/2/T-ERK1/2), in response to PDGF (10 ng/ml) for 10 min in VSMC cultured from VSMC-specific heterozygous ROCK2-deficient (ROCK2$^{+/-}$ VSMC) and littermate control mice (LM VSMC). (**B**) Quantitative analysis of ERK activity in ROCK2$^{+/-}$ VSMC and LM VSMC (n=4 each). (**C**) Representative immunoblots of ERK activity in response to PDGF in VSMC cultured from VSMC-specific ROCK2-overexpressing transgenic mice (ROCK2-Tg VSMC) and wild-type littermate control mice (CTL VSMC). (**D**) Quantitative analysis of ERK activity in ROCK2-Tg VSMC and CTL VSMC (n=4). Results are expressed as mean ± SEM.

Supplemental Figure VII

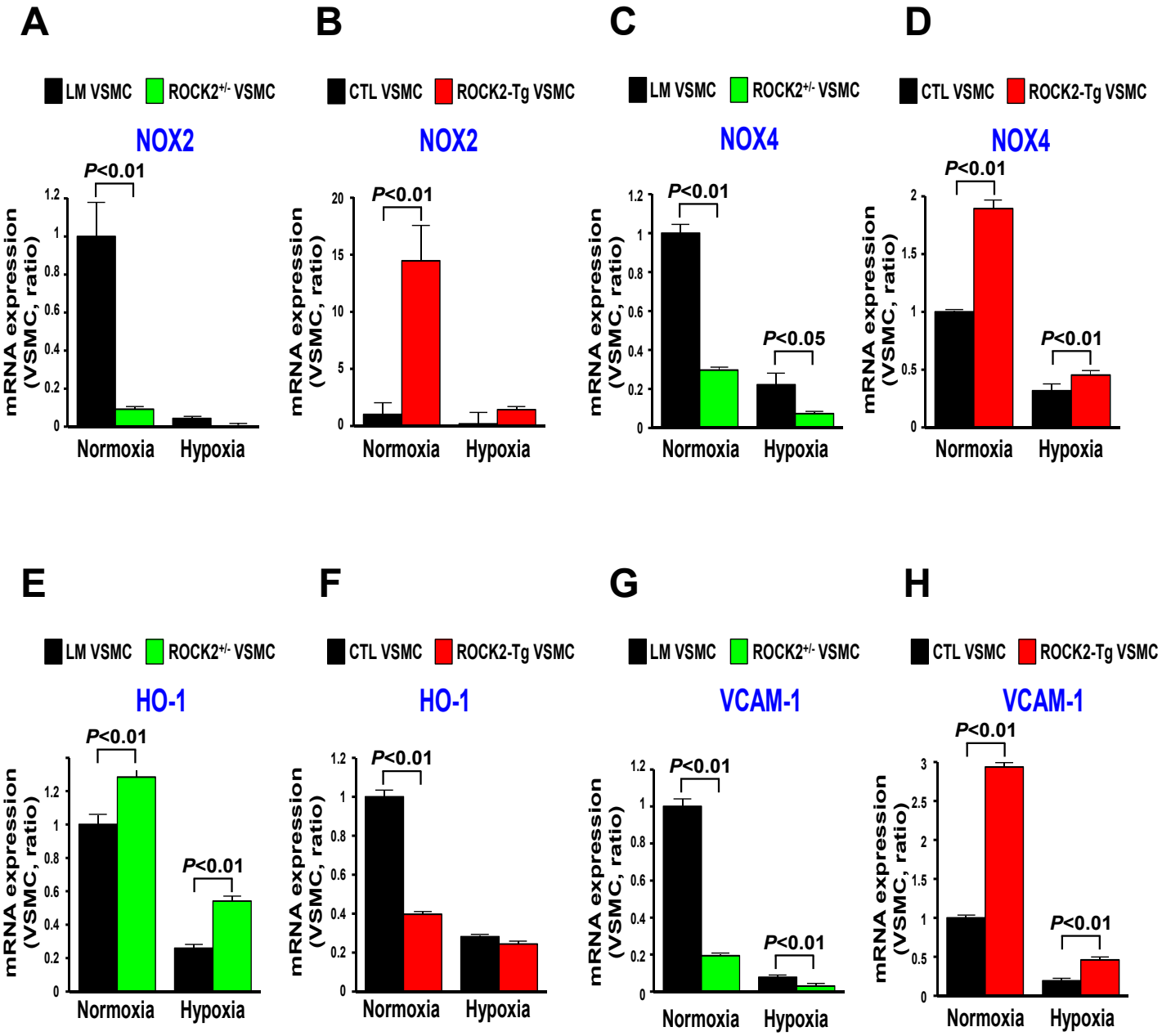

Supplemental Figure VII. ROCK2 mediates hypoxia-induced oxidative stress and an adhesion ligand in mice in vitro

Quantitative analysis of NOX2, NOX4, HO-1 and VCAM-1 mRNA expression stimulated by room air (normoxia) or 2% oxygen (hypoxia) for 24h in VSMC cultured from (**A, C, E, G**) VSMC-specific heterozygous ROCK2-deficient mice (ROCK2$^{+/-}$ VSMC) and littermate control mice (LM VSMC) and from (**B, D, F, H**) VSMC-specific ROCK2-overexpressing transgenic mice (ROCK2-Tg VSMC) and wild-type littermate control mice (CTL VSMC) (n=3-6, each). The mRNA levels of target genes were divided by those of GAPDH. Results are expressed as mean ± SEM.

Supplemental Figure VIII

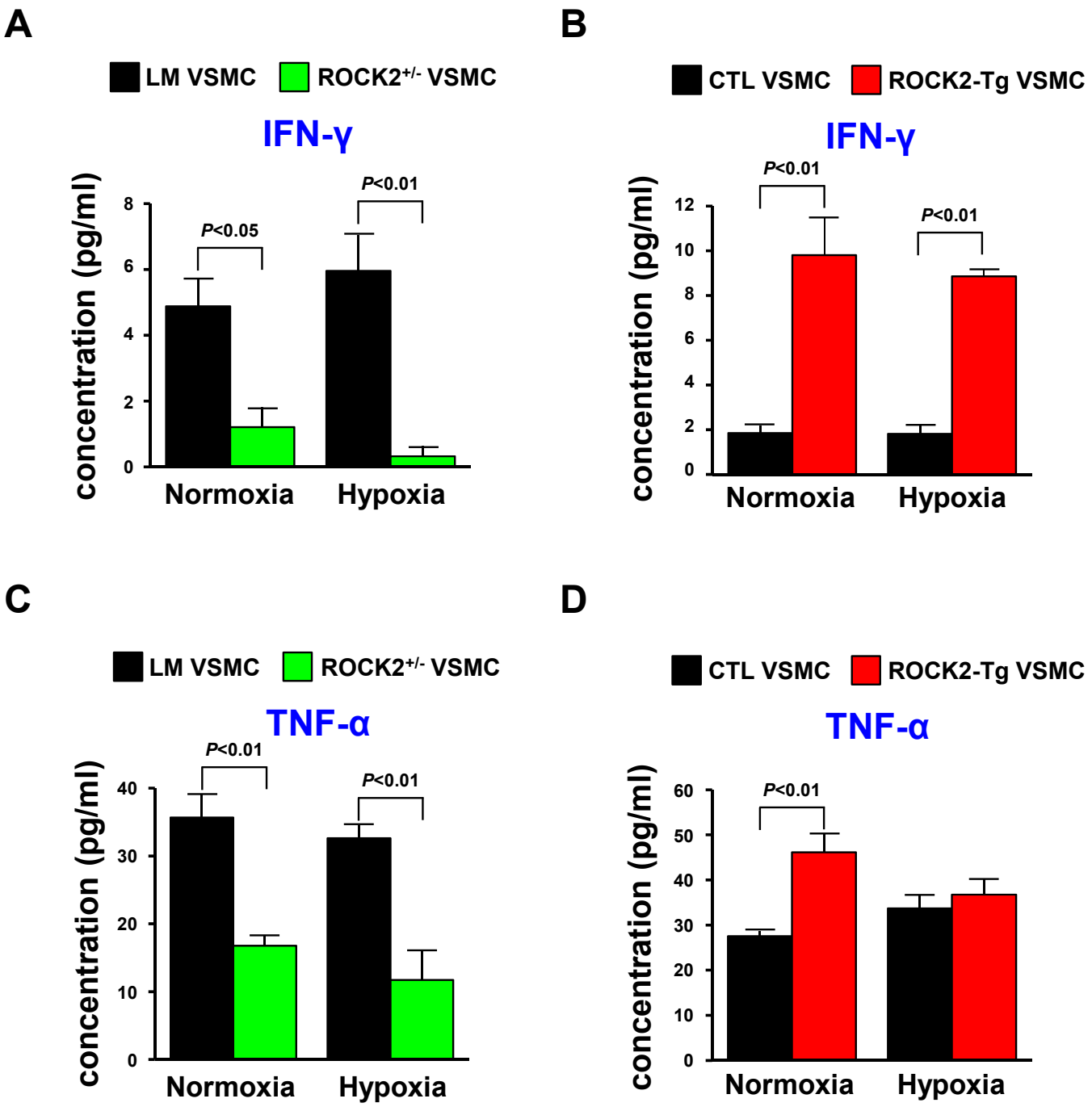

Supplemental Figure VIII. ROCK2 mediates hypoxia-induced inflammatory response in mice in vitro

Analysis of cytokine secretion in the conditioned medium stimulated by room air (normoxia) or 2% oxygen (hypoxia) for 24h from VSMC cultured from (**A, C**) VSMC-specific heterozygous ROCK2-deficient mice (ROCK2$^{+/-}$ VSMC) and littermate control mice (LM VSMC) and from (**B, D**) VSMC-specific ROCK2-overexpressing transgenic mice (ROCK2-Tg VSMC), and wild-type littermate control mice (CTL VSMC) (n=5 each). Results are expressed as mean ± SEM.

Supplemental Figure IX

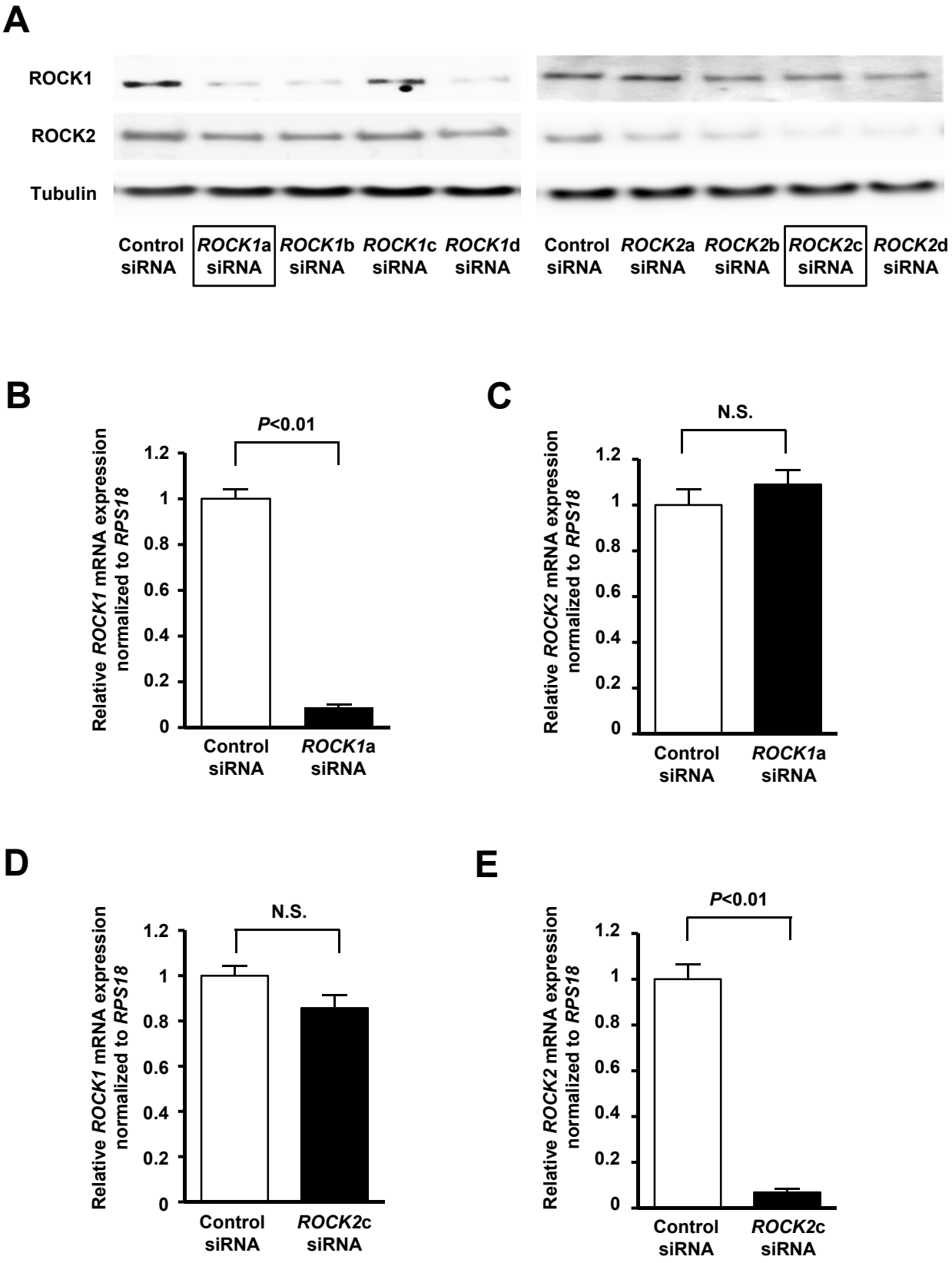

Supplemental Figure IX. Effective knockdown of ROCK1 and ROCK2 expression in PASMC from a patient with IPAH (IPAH-PASMC).

(**A**) Representative immunoblots of ROCK1 and ROCK2 in IPAH-PASMC. IPAH-PASMC were transfected with 4 kinds of siRNA duplexes targeted to *ROCK1* (*ROCK1*a, b, c, and d) and *ROCK2* (*ROCK2*a, b, c, and d), respectively. *ROCK1*a-siRNA and *ROCK2*c-siRNA showed the most effective knockdown of each protein and were adopted in the present study. (**B**, **C**) Quantitative analysis of *ROCK1* and *ROCK2* mRNA in IPAH-PASMC transfected with *ROCK1*a-siRNA. (**D**, **E**) Quantitative analysis of *ROCK1* and *ROCK2* mRNA in IPAH-PASMC transfected with *ROCK2*c-siRNA. Results are expressed as mean ± SEM.

Supplemental Figure X

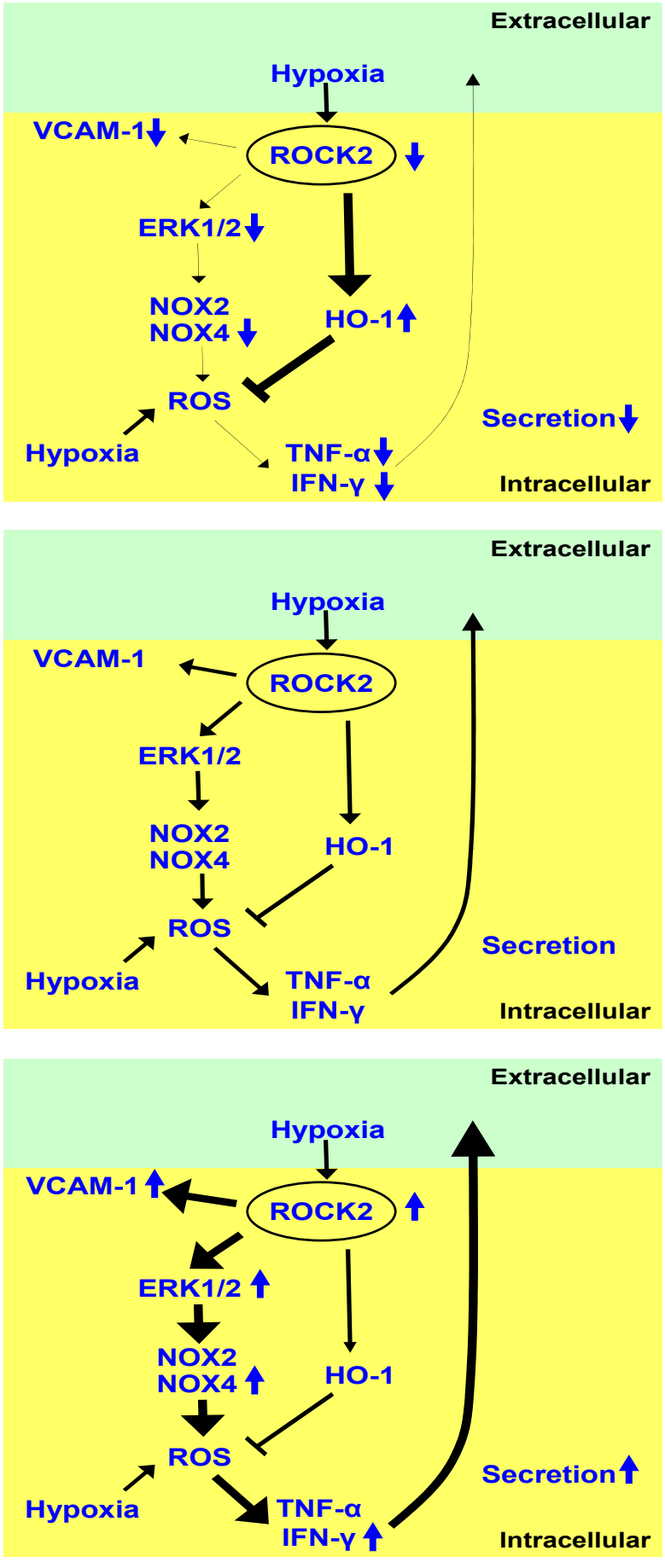

Supplemental Figure X. ROCK2 in VSMC mediates cell proliferation and migration through oxidative stress and inflammatory cytokines.

Supplemental Tables

Supplemental Table I. Hematological Parameters in Littermate Control (LM) and VSMC-specific ROCK2-deficient (ROCK2$^{+/-}$) Mice under Normoxia and after 4-week Hypoxia

Hematological variables	Normoxia		Hypoxia	
	LM (n=10)	ROCK2$^{+/-}$ (n=10)	LM (n=10)	ROCK2$^{+/-}$ (n=10)
White blood cells ($\times10^3$/mm^3)	5.6±1.1	5.0±0.2	6.0±0.3	5.5±0.5
Red blood cells ($\times10^6$/mm^3)	10.2±0.4	10.3±0.3	13.1±0.5**	13.2±0.2**
Hematocrit (%)	48.3±1.8	49.2±1.5	63.6±1.6**	65.3±0.6**
Hemoglobin (g/dl)	15.1±0.5	15.5±0.3	19.5±0.5**	19.9±0.2**
Platelets ($\times10^3$/mm^3)	629±65	581±27	417±23**	425±22*

Results are expressed as mean ± SEM. Comparisons were performed using one-way ANOVA. *P<0.05, **P<0.01 vs. normoxia in each group.

Supplemental Table II. Hematological Parameters in Littermate Control (CTL) and VSMC-specific ROCK2-overexpressing (ROCK2-Tg) Mice under Normoxia and after 4-week Hypoxia

Hematological variables	Normoxia		Hypoxia	
	CTL (n=10)	ROCK2-Tg (n=10)	CTL (n=10)	ROCK2-Tg (n=10)
White blood cells ($\times 10^3/mm^3$)	4.4±0.3	4.3±0.3	4.9±0.6	5.0±0.5
Red blood cells ($\times 10^6/mm^3$)	10.0±0.2	10.4±0.2	13.3±0.3**	13.3±0.3**
Hematocrit (%)	48.4±1.3	50.7±1.3	65.6±0.7**	66.5±0.9**
Hemoglobin (g/dl)	15.1±0.3	15.9±0.3	20.6±0.4**	20.8±0.4**
Platelets ($\times 10^3/mm^3$)	611±26	647±49	392±26**	405±34**

Results are expressed as mean ± SEM. Comparisons were performed using one-way ANOVA. **$P<0.01$ vs. normoxia in each group.

Materials and Methods

Generation of VSMC-specific ROCK2-deficient Mouse

For generation of VSMC-specific ROCK2-deficient mice, *SM22α* promoter-driven Cre recombinase transgenic mice were crossed to *Rock2*-floxed mice. *SM22α* promoter-driven Cre recombinase transgenic mice, which express Cre primarily in VSMC, were purchased from the Jackson Laboratory. For generation of *Rock2*-floxed mice, the mouse genomic DNA was obtained from a C57BL/6 bacterial artificial chromosome (BAC) clone (RPCI23). The targeting vector was generated by flanking exon 3 of the mouse *Rock2* gene with 2 loxP sites to induce Cre-mediated deletion of exon 3. The single loxP site is inserted 5' to exon 3 and loxP/FRT-flanked neomycin (Neo) resistance cassette was inserted 3'to exon 3 (**Figure IA in the online-only Data Supplement**). The targeting construct was linearized and electroporated into C57BL/6 × 129/SvEv hybrid embryonic stem cells (inGenious Targeting Laboratory). Positive ES cells containing target vectors were identified by PCR and Southern bot analysis and microinjected into C57BL/6J blastocysts to generate chimeras. The resulting male chimeras were crossed to wild-type female C57BL/6J mice to generate heterozygous *Rock2*-floxed mice (*Rock2*$^{+/flox}$). The F1 agouti *Rock2*$^{+/flox}$ mice genotyped by PCR were crossed to *Flp1* transgenic mice purchased from the Jackson Laboratory to remove the Neo cassette by the FLP-mediated recombination. To generate vascular smooth muscle cell-specific ROCK2-deficient mice, *Rock2*-floxed mice were crossed to the *SM22α*-Cre transgenic mice (*SM22*-Cre$^{+/-}$). The resulting *SM22*-Cre$^{+/-}$/*Rock2*$^{+/flox}$ mice (ROCK2$^{+/-}$) were used for all experiments because *SM22*-Cre$^{+/-}$/*Rock2*$^{flox/flox}$ mice (ROCK2$^{-/-}$) were embryonically lethal and then *SM22*-Cre$^{-/-}$/*Rock2*$^{+/flox}$ mice (LM) were used as littermate control mice, identified by PCR on genomic DNA isolated from the tail biopsies (**Figure IB in the online-only Data Supplement**). Each genotype of mice was backcrossed to C57BL/6 mice for the N8 generation. The primers used to genotype transgenic mice are as follows; SM22α promoter Cre, 5'- GTTCGCAAGAACCTGATGGACA -3' and 5'- CTAGAGCCTGTTTTGCACGTTC -3'; LoxP *Rock2*, 5'- TAAGACCTAGAGCACAGTC -3' and 5'- GGATTTGTTGGCACATCACTGAGTACC -3'.

Generation of VSMC-specific ROCK2-overexpressing Mouse

For generation of VSMC-specific overexpression of ROCK2 in transgenic mice, the targeting vectors used in this study were constructed by BAC recombineering technology using Red/ET recombination system (Gene Bridges).[1] The mouse *Rock2* BAC clone, RP23-215G12, and the rat *SM22* BAC clone, CH230-326P20 was searched by GenBank database at NCBI and obtained from BACPAC Resources Center at Children's Hospital Oakland Research Institute. Using Red/ET recombination technology, the genomic coding sequence of the mouse *Rock2* gene was removed precisely from the BAC clone. Similarly, the genomic coding sequence of rat *SM22* was removed from the BAC clone and replaced by the subcloned mouse *Rock2*

gene fragment to construct a *SM22*/*Rock2* BAC clone. BAC modification was confirmed by sequencing. The linearized *SM22α*/*Rock2* DNA fragment was microinjected into oocytes isolated from C57BL/6J stain (Charles River Laboratories). Oocytes that survived injection were transferred into oviducts of pseudo-pregnant mothers. Transgenic mice were identified by both PCR and Southern analysis with genomic DNA isolated from tail biopsies (**Figure IC in the online-only Data Supplement**). Each genotype of mice was backcrossed to C57BL/6 mice for the N8 generation. The primers used to genotype transgenic mice are as follows; 5'-CCGACCGATATCTAAGACCTTGT-3' and 5'-TCCACTCTGGAACCTGGGTCT-3'. VSMC-specific ROCK2-overexpressing mice that were heterozygous for mouse *Rock2* expressed by the *SM22α* promoter (ROCK2-Tg) and wild-type littermate control mice not expressing the transgene (CTL) were used for all experiments.

Harvesting of Mouse Aortic VSMC

Mouse aortic VSMC were cultured from each genotype of 20-25 g male mice and maintained in Dulbecco's modified Eagle's medium (DMEM) containing 10% fetal bovine serum (FBS) (10099-141; Invitrogen) at 37˚C in a humidified atmosphere of 5% CO_2 and 95% air as previously described. Passage 4 to 7 VSMC at 70-80% confluence was used for experiments.[2]

Human Lung Samples

Lung tissue samples were obtained from patients with IPAH at the time of lung transplantation or from control patients at the time of thoracic surgery for lung cancer at a site from the tumor margins. Before the surgery, all patients provided their written consent to the use of their lung tissues for the investigational research for IPAH. Ethics approval was obtained from the Ethics Committee of Tohoku University Graduate School of Medicine.

Isolation of Human PASMC

Small pulmonary arteries were also obtained at the time of lung transplantation from 5 patients with IPAH (3 males and 2 females; mean age, 27±7 years; age range 11-50 years). Pulmonary arterial smooth muscle cells from IPAH patients (IPAH-PASMC) were isolated from pulmonary arteries smaller than 1.5 mm in outer diameter as previously described.[3] PASMC from control subjects without pulmonary hypertension (2 males and 3 females; mean age, 39±10 years; age range 2.5-58 years) were purchased from Lonza Biologics Inc. (CC-2581; lot 13981, lot 191775, lot 7F3559, lot 7F3560 and lot 7F3602). PASMC were cultured in DMEM containing 10% FBS at 37˚C in a humidified atmosphere of 5% CO_2 and 95% air. IPAH-PASMC from a male 14-year-old IPAH patient were used for a series of

experiments using siRNA. Passage 4 to 7 VSMC at 70-80% confluence was used for experiments.

Animal Experiments

8-week old adult male mice were exposed to hypoxia or normoxia for 4 weeks. Hypoxic mice were housed in an acrylic chamber with non-recirculating gas mixture of 10% O_2 and 90% N_2 by adsorption-type oxygen concentrator to utilized exhaust air (Teijin), while normoxic mice were housed in room air (21% O_2), under a 12h light-dark cycle.[4] As compared with 21% O_2, acute 10% O_2 hypoxic condition significantly decreased arterial O2 (PaO2) from 103±6 to 56±7 mmHg in mechanically ventilated, anesthetized adult wild-type mice ($P<0.01$, n=4 each) and is supposed to reflect moderate to severe PH condition in humans. In the present study, the assessment of PH and histological evaluations for each genotype of mice was performed after 4 weeks of hypoxic or normoxic exposure. All protocols were approved by the Tohoku University Animal Care and Use Committee.

Hemodynamic Measurements

After 4 weeks of maintenance in hypoxia or normoxia, mice were anesthetized with isoflurane (1.0-1.5%). Mice were laid supine position with all legs taped to electrocardiogram electrodes for heart rate monitoring. For right heart catheterization, a 1.2-F pressure catheter (Scisense Inc.) was inserted in the right jugular vein and advanced into the RV (right ventricle) to measure the following parameters; RV systolic pressure (RVSP), RV end-diastolic pressure (RVEDP), and peak rates of RV pressure development (RV dP/dt max) and relaxation (RV dP/dt min). For left heart catheterization, the catheter was inserted in the left carotid artery and advanced into the ascending aorta, and then into the left ventricle (LV) to measure the following parameters; blood pressure, LV systolic pressure (LVSP), LV end-diastolic pressure (LVEDP), and peak rates of LV pressure development (LV dP/dt max) and relaxation (LV dP/dt min). All data were analyzed using the PowerLab data acquisition system (AD Instruments), and averaged from 10 sequential beats. These measurements were performed within 1 h after hypoxic exposure.

Histological Analysis

Murine and human lung samples were fixed in 10% formaldehyde and embedded in paraffin. 3 μm sections of fixed murine left lung tissue were stained with Elastica-Masson and assessed by light microscopy (BX51, Olympus). Pulmonary vascular remodeling was evaluated by measuring medial wall thickness of distal pulmonary vessels (15-80 μm of external diameter). Medial wall thickness was expressed as follows; percent wall thickness = [(WT1+WT2)/external diameter] × 100, where WT1 was measured at one point of the vessel and WT2 at the diametrically opposite point.[5] For each mouse, at least 100 vessels were measured at a magnification of × 400 in a blind manner.

Right Ventricular Hypertrophy Measurements

Formaldehyde-fixed dry hearts were dissected and the right ventricular wall was removed from the left ventricle and septum. A ratio of the right ventricle to the left ventricle plus septum weight [RV/(LV + S)] was calculated to determine the extent of right ventricular hypertrophy.

Blood Analysis

Blood (0.5-1.0 ml) was obtained from mice by right ventricle puncture when they were euthanized. Blood cell counts were determined using a multi-automatic blood cell counter for animals (MICROS abc LC-152, HORIBA Ltd.).

Immunohistochemistry

Serial sections with 3-μm thickness were used for all immunohistochemical experiments. Formaldehyde-fixed paraffin sections were incubated with primary antibody at 4˚C. Immunohistochemistry was performed using the biotin-avidin complex method (Histofine SAB-PO(M) kit/SAB-PO(R) Kit, Nichirei Co.) according to the manufacturer's protocol. Antigen retrieval was performed for all primary antibodies using Target Retrieval Solution (Dako). The primary antibodies used were anti-ROCK1 (ab45171; Abcam), anti-ROCK2 (HPA007459; Sigma), anti-phosopho-ERK 1/2 (#4370; Cell Signaling), anti-αSMA (M0851; Dako), anti-CD45 (550539; BD Biosciences) and anti-Ki67 (ab66155; Abcam). Counter staining was performed by resorcin-fuchsin for elastic fibers and hematoxylin for nuclei. Negative control experiments were performed with the isotype-matched IgG. Slides were viewed with a light microscope (BX51, Olympus) and analyzed by DP Controller and DP Manager software (Olympus).

Measurement of Inflammatory and Proliferating Vascular Cells in the Medial Wall of Pulmonary Arteries

The number of inflammatory and proliferating cells was determined by immunostaining with anti-CD45 and anti-Ki67 antibody, respectively. The number of CD45- and Ki67-positive cells was counted as immunostained cells per distal pulmonary vessels (15-80 μm of external diameter). Pulmonary vessels were identified by Resorcin-fuchsin co-staining for the elastic lamina. For each mouse, at least 30 vessels were randomly measured at a magnification of × 400 in a blind manner.

Western Blot Analysis

Protein was extracted from mouse lung tissues, mouse aorta, mouse aortic VSMC and human PASMC. To evaluate ROCK expression in the media of aorta from ROCK2$^{+/-}$ and LM mice, isolated aorta were stripped of the endothelium by gently rubbing the inner surface with

cotton string. The same amount of extracted protein was loaded on sodium dodecyl sulfate-polyacrylamide gel electrophoresis (SDS-PAGE) gel and transferred to polyvinylidene difluoride (PVDF) membranes (GE Healthcare), following blocking by 1 h at room temperature. The membranes were immunoblotted by using anti-ROCK1 (611136; BD Biosciences), anti-ROCK2 (610623; BD Biosciences), anti-MBS (612165; BD Biosciences), anti-phospho-specific threonine 696 MBS (ABS45; Millipore), anti-phospho-specific threonine 853 MBS (#4563; Cell Signaling), anti-ERK 1/2 (ab17942; Abcam), anti-phosoho-ERK 1/2 (#4377; Cell Signaling), and anti-α-tubulin (T9026; Sigma). The regions containing proteins were visualized by the enhanced chemiluminescence system (ECL Western Blotting Detection Kit, GE Healthcare) as previously described.[6] Densitometric analysis was performed by the Image J Software (NIH).

RNA Isolation and Real-time PCR

Isolation of total RNA from mouse VSMC and human PASMC was performed using the RNeasy Plus Mini Kit (Qiagen) according to the manufacturer's protocol. Total RNA was converted to cDNA using PrimeScript RT Master Mix (Takara). Primers for human *ROCK1* (Primer Set ID: HA091644), *ROCK2* (Primer Set ID: HA175879) and ribosomal protein S18 (*RPS18*) (Primer Set ID: HA067807) and for murine *Nox2* (Primer Set ID: MA119744) and *Gapdh* (Primer Set ID: MA050371) were purchased from Takara. Primers for murine *Rock1* (Assay ID: Mm00485745_m1), *Rock2* (Assay ID: Mm01270843_m1), *Nox4* (Assay ID: Mm00479246_m1), *Vcam1* (Assay ID: Mm01320970_m1), *Ho1* (Assay ID: Mm00516005_m1), *Gapdh* (Assay ID: Mm99999915_g1) and ribosomal protein S18 (*Rps18*) (Assay ID: Mm02601777_g1) from Life Technology. Quantitative real-time PCR on the CFX 96 Real-Time PCR Detection System (Bio-Rad) was performed using SYBR premix Ex Taq (Takara) with SYBR Green I for human and murine samples and SsoFast Probes Supermix (Bio-Rad) with TaqMan Probe for murine samples. The Ct value analyzed by the CFX Manager Software (version2.0, Bio-Rad) for all samples was normalized with housekeeping gene ribosomal protein S18 and the relative fold change was computed by ΔΔCt method.

Transfection of Human PASMC with siRNA

Multiple siRNA duplexes for *ROCK1* and *ROCK2* were purchased from Qiagen. A functional non-targeting siRNA that was bioinformatically designed by Qiagen was used as a control (control siRNA) (AllStars Negative Control siRNA; #102780). Human PASMC from a patient with IPAH were transfected with HiPerFect Transfection Reagent (Qiagen) with either 30 nM control siRNA or 30 nM siRNA specific for *ROCK1* (*ROCK1*-siRNA) (#SI02622095) and *ROCK2* (*ROCK2*-siRNA) (#SI02223746) according to the manufacturer's protocol. Sufficient down-regulation of *ROCK1* and *ROCK2* was achieved 72 h after transfection. Dual transfection for 72 h with both 30 nM *ROCK1*-siRNA and 30 nM

ROCK2-siRNA (dual *ROCK1*/*2*-siRNA) also showed sufficient knockdown of *ROCK1* and *ROCK2* simultaneously.

Cell Proliferation Assay

Mouse aortic VSMC were seeded in 24-well plates (20,000 cells/well) in DMEM without FBS and starved for 24 h, then stimulated with 10% FBS or 0.1% FBS for up to 5 days. Human PASMC were also seeded in 24-well plate (20,000 cells/well) in DMEM without FBS and starved for 24 h, then transfected with siRNA and stimulated with 10% FBS or 0.1%FBS up to 5 days. Medium was changed at day 3, and cells were counted at day 1, 3 and 5. Each value was derived from 3 independent experiments performed in triplicate.

Scratch Assay

Confluent mouse aortic VSMC in 60-mm dishes were starved for 24 h. Human PASMC transfected with siRNA for 72 h were also seeded confluently in 60 mm dishes and starved for 24 h. Then, a linear wound (600 μm in width) was made through the center of plate using a pipette tip and medium was replaced with DMEM with 0.1% FBS. 12 h after scraping, dishes were photographed and the maximum distance of smooth muscle cell migration was analyzed by a phase-contrast microscope.[7]

Modified Boyden Chamber Migration Assay

Cell migration assay was performed using a 24-well plate and Chemotaxicell (8μm pore size, Kurabo). The membrane of Chemotaxicell was coated with 0.3 mg/ml of collagen I (Nitta Gelatin). 50,000 cells were starved for 24 h, and plated at the upper chamber. 10ng/ml PDGF-BB (220-BB; R&D systems) was added to the lower chamber and incubated for 6 h. The membrane on the lower surface was subsequently fixed with 70% ethanol and stained with hematoxylin and eosin. The migrated cells on underside of membrane were counted manually in 10 random microscopic fields (×400).[8]

Measurement of cytokines

Confluent mouse aortic VSMC were serum starved for 24 h and then were stimulated with normoxia (21% O_2) or hypoxia (2% O_2). 24h after stimulation, the conditioned medium was collected and centrifuged for 10 min at 800*g* to remove cell debris. Then, the medium was concentrated 100 fold with a Centricon Plus-20 filter (Millipore Corp.) to yield concentrated conditioned medium.[2] The conditioned medium was analyzed for inflammatory cytokines by Bio-Plex bead-based cytokine assay (Bio-Rad) according to the manufacture's protocol. Concentrations of cytokines were calculated from the standard curve with Bio-Plex Manager 6.0 software (Bio-Rad).

Statistical Analysis

All data are shown as mean ± SEM. Comparisons of parameters were performed with the unpaired Student's t-test or ANOVA followed by Tukey's HSD test for multiple comparisons. Statistical significance was evaluated with JMP 9 (SAS Institute Inc, Cary, NC). A *P* value of <0.05 was considered to be statistically significant.

References

1. Fujita E, Tanabe Y, Shiota A, Ueda M, Suwa K, Momoi MY, Momoi T. Ultrasonic vocalization impairment of Foxp2 (R552H) knockin mice related to speech-language disorder and abnormality of Purkinje cells. *Proc Natl Acad Sci U S A.* 2008;105:3117-3122.
2. Satoh K, Matoba T, Suzuki J, O'Dell MR, Nigro P, Cui Z, Mohan A, Pan S, Li L, Jin ZG, Yan C, Abe J, Berk BC. Cyclophilin A mediates vascular remodeling by promoting inflammation and vascular smooth muscle cell proliferation. *Circulation.* 2008;117:3088-3098.
3. Ogawa A, Nakamura K, Matsubara H, Fujio H, Ikeda T, Kobayashi K, Miyazaki I, Asanuma M, Miyaji K, Miura D, Kusano KF, Date H, Ohe T. Prednisolone inhibits proliferation of cultured pulmonary artery smooth muscle cells of patients with idiopathic pulmonary arterial hypertension. *Circulation.* 2005;112:1806-1812.
4. Satoh K, Kagaya Y, Nakano M, Ito Y, Ohta J, Tada H, Karibe A, Minegishi N, Suzuki N, Yamamoto M, Ono M, Watanabe J, Shirato K, Ishii N, Sugamura K, Shimokawa H. Important role of endogenous erythropoietin system in recruitment of endothelial progenitor cells in hypoxia-induced pulmonary hypertension in mice. *Circulation.* 2006;113:1442-1450.
5. Tawara S, Fukumoto Y, Shimokawa H. Effects of combined therapy with a Rho-kinase inhibitor and prostacyclin on monocrotaline-induced pulmonary hypertension in rats. *J Cardiovasc Pharmacol.* 2007;50:195-200.
6. Nochioka K, Tanaka S, Miura M, Zhulanqiqige do E, Fukumoto Y, Shiba N, Shimokawa H. Ezetimibe improves endothelial function and inhibits Rho-kinase activity associated with inhibition of cholesterol absorption in humans. *Circ J* 2012;76:2023-2030.
7. Liang CC, Park AY, Guan JL. In vitro scratch assay: a convenient and inexpensive method for analysis of cell migration in vitro. *Nat Protoc.* 2007;2:329-333.
8. Goncharova EA, Goncharov DA, Krymskaya VP. Assays for in vitro monitoring of human airway smooth muscle (ASM) and human pulmonary arterial vascular smooth muscle (VSM) cell migration. *Nat Protoc.* 2006;1:2933-2939.